PC-BASED ULTRASONIC RADAR DEMONSTRATOR FOR SPORTS APPLICATIONS

Presented by:
Ian Edwards

Prepared for:
Dr Yunus Abdul Gaffar

October 22, 2021

Submitted to the Department of Electrical Engineering at the University of Cape Town in partial fulfilment of the academic requirements for the degree of BSC Electrical and Computer Engineering.

Abstract

The use of technology in sports to enhance performance has been growing in popularity in the 21st century. Radar technologies in general are often expensive and thus inaccessible both in sports applications and for research. This research project aims to develop a well packaged ultrasonic radar demonstrator that can reliably estimate the velocity of sports balls for demonstration and research purposes, and compare its performance to that of an audio system and S-Band radar system. The focus is on the hardware design, initial signal processing and user friendliness of the radar demonstrator. The hardware design is detailed along with the signal processing techniques and user application design. Various tests are then carried out in order to characterize the performance of the ultrasonic system in comparison with the performance of an audio SONAR system and RF system. Indoor and outdoor tests are carried out along with video recordings from which a baseline of velocity values could be computed against which to compare radar data.

The ultrasonic system is shown to be more effective at detecting low speed sporting objects in comparison with an audio SONAR system, and is able to detect large sports balls like footballs and basket balls at a maximum distance of 8.5 metres. Whilst both the audio and ultrasonic systems did not perform as well as the S-Band coffee can radar system, they provide low-budget (R856.00) accessible solutions for simple sports monitoring applications as well as providing a demonstrator system to gain hands-on experience with radar technology for learning and research purposes. Recommendations are given for improvement with optimal audio transmit frequencies being experimentally identified, and methods to increase the bandwidth of the ultrasonic system and thus the maximum velocities detectable.

Acknowledgments

I would like to express my sincere gratitude to my supervisor, Dr Yunus Abdul Gaffar, for his wisdom, patience and guiding expertise throughout the project. His passion for learning and research is shown through his eagerness to help students.

Various masters students in the department were pivotal in achieving progress in various areas of my project namely Ndumiso Khumalo, Lawrence Stanton and Michael Katsoulis. They showed such readiness and friendliness in assisting with various academic questions, and thus showed me the collaborative environment of research.

I have so much appreciation for my family and friends who throughout my studies and final project always celebrated my little successes along the way, walked this journey with me and always put utmost faith in my abilities. My successes are highly shaped by their support.

Ultimately I commit this project all to the glory of God who has loved and shaped me throughout my life and made His presence known.

Plagiarism Declaration

1. I know that plagiarism is wrong. Plagiarism is to use another's work and pretend that it is one's own.
2. I have the IEEE convention for citation and referencing. Each contribution to, and quotation in, this final year project report from the work(s) of other people, has been attributed and has been cited and referenced.
3. This final year project report is my own work.
4. I have not allowed, and will not allow, anyone to copy my work with the intention of passing it off as their own work or part thereof.

.....

Ian Edwards
October 22, 2021

Contents

Abstract i

Acknowledgments ii

Plagiarism Declaration iii

Table of Contents iv

List of Figures vii

List of Tables x

Chapter 1: Introduction 1

1.1 Background and Motivation 1
1.2 Problem Statement 3
1.3 Objectives 4
1.4 Contributions 6
1.5 Requirements and testing procedures 6
1.5.1 User Requirements 6
1.5.2 Technical Specifications 8
1.5.3 Acceptance Test Procedures (ATPs) 9
1.6 Scope and Limitations 10
1.7 Outline 10

Chapter 2: Literature Review 11

2.1 History of RADAR 11

2.2 Fundamentals of RADAR 12
2.3 The Doppler effect and Doppler Radar 15
2.4 RADAR versus SONAR 17
2.5 Important signal processing concepts 19
2.6 Existing applications of ultrasonic systems 20
2.6.1 Ultrasound in medicine 20
2.6.2 Ultrasound in Deep learning and gesture recognition 21
2.6.3 Ultrasound in driving-aid and active safety systems 21
2.6.4 Ultrasound for indoor mapping 22
2.6.5 Ultrasound for level measurement and industrial applications 23
2.7 Existing Sports tracking-velocity Devices 24
2.7.1 Types of sensors used in various sports applications 24
2.7.2 Application of RADAR in sports 27
2.8 Characterizing the performance of a RADAR system 28
2.9 Critical Review 28

Chapter 3: Methodology **30**
3.1 Methodology Overview 30
3.2 Project Phases 31
3.3 Data collection and logging 32
3.4 Experiment Design 32
3.4.1 Ideal Transmit Frequency Experiment 33
3.4.2 Noise Threshold 33
3.4.3 Algorithm Tests 34
3.4.4 RCS Tests 35
3.4.5 Range Tests 36

Chapter 4: Design **37**
4.1 System Design Overview 37
4.2 Hardware Design 38
4.2.1 Data acquisition Device - ADC/DAC 38
4.2.2 MIT Coffee Can RADAR System 40

4.2.3 Audio RADAR System 41
4.2.4 Ultrasonic System Design 42
4.2.5 Receiver Simulations and results 52
4.2.6 Enclosure Design 57
4.3 Signal Processing Design 61
4.4 GUI Design and data logging 68

Chapter 5: Results **71**
5.1 Experiments and Results 71
5.1.1 Experimental Setup 71
5.1.2 Experiment Walkthrough 74
5.1.3 Results Summary 79
5.2 Discussion 80
5.2.1 Frequency Tests 80
5.2.2 Noise Threshold 80
5.2.3 Optimal Algorithm Tests 81
5.2.4 Ball Size (RCS) Tests 81
5.2.5 Range Tests 82
5.3 Acceptance Test Procedures Evaluation 83

Chapter 6: Conclusions **85**
6.1 Conclusions 85
6.2 Future Work 86
6.2.1 Hardware 86
6.2.2 Software 87
6.2.3 RADAR system 87
6.2.4 Signal Processing 88
6.2.5 Experimentation 88

Bibliography **89**

Appendix A: Supporting Data **92**

List of Figures

1.1 An illustration of the interaction between a moving object and an EM wave [7] 2

2.1 Basic RADAR system [1] 13
2.2 Pulsed Radar waveform [1] 14
2.3 An illustration of the interaction between a moving object and an EM wave [7] 16
2.4 An illustration of the Doppler shift and how it relates to the radial component of a target's velocity [1] 17
2.5 Hawk-Eye system and its cameras in a stadium [22] 26
2.6 Compact PocketRadar device used to measure ball speed [2] 27

4.1 System overview showing the system's subsystems 37
4.2 MIT Coffee Can RADAR system setup with the above components [26] 40
4.3 SP-HF160 speakers used as the transmitter in the audio RADAR system 41
4.4 Havit HV-M80 microphone used as the receiver in the audio RADAR system 41
4.5 Overview of the design of the ultrasonic system 42
4.6 Frequency Response of ultrasonic barrel transducers obtained experimentally 43
4.7 Transmitter circuit design 47
4.8 LTSpice simulated Tx 1st stage of BPF frequency response 48
4.9 LTSpice simulated transmitter circuit overall frequency response . . . 48
4.10 Tx 1st stage of BPF frequency response 49
4.11 Transmitter circuit overall frequency response 49

4.12 Receiver circuit design 51
4.13 LTSpice simulated Rx 1st stage of BPF frequency response 52
4.14 LTSpice simulated receiver circuit overall frequency response 52
4.15 Rx 1st stage of BPF frequency response 53
4.16 Receiver circuit overall frequency response 53
4.17 Receiver circuit output in response to a 0.5 Vp 40 kHz signal input . 54
4.18 Receiver circuit clipping action on too large an input signal 54
4.19 Mini car charger power bank 55
4.20 Comparison of custom dual rail supply circuitry versus Lawrence Stanton's PCB 56
4.21 Power circuitry design to obtain +-12V from 12V power bank 57
4.22 Fusion 360 generated technical drawing of the designed enclosure . . . 59
4.23 Interior view of the finished hardware system 60
4.24 Front view of the finished hardware system 60
4.25 Top view of the finished hardware system 61
4.26 Signal processing flow chart 62
4.27 Key steps in signal processing 63
4.28 Bandpass filter used to remove DC components received in the signal 64
4.29 Notch filter used to remove 40 kHz clutter in the received signal . . . 65
4.30 Raw STFT output before thresholding and smoothing, plotted as a spectrogram 67
4.31 MATLAB pspectrum output 68
4.32 Normalized STFT output plotted as a spectrogram of velocity versus time 68
4.33 Developer_Demonstrator application interface 69
4.34 RADAR Demonstrator user interface 70

5.1 Indoor test setup 72
5.2 Outdoor test setup 73
5.3 GUI setup for experiments 74
5.4 Received signal before thresholding, with custom STFT versus MATLAB "pspectrum" output 75

5.5 Normalized custom spectrogram output 76
5.6 Normalized pspectrum output 76
5.7 Velocity metrics outputted from both processing methods 77

A.1 S-Band Radar football test results 94
A.2 S-Band Radar tennis ball test results 94

List of Tables

1.1 Table of User Requirements 7
1.2 Table of Technical Specifications 8
1.3 Table of Acceptance Test Procedures (ATPs) 9

4.1 Table of sound card specifications 39
4.2 Table of Transmitter (SP-HF160 speakers) Specifications 41
4.3 Table of Receiver (Havit HV-M80 microphone) Specifications 41
4.4 Table of ultrasonic barrel transmitter specifications 43
4.5 Table of ultrasonic barrel receiver specifications 43
4.6 Table of LT1214CN operational amplifier specifications 45
4.7 Table of Technical Specifications 55

5.1 Table of frequency tests 79
5.2 Table of range tests 79
5.3 Table of indoor test results 79
5.4 Table of outdoor (slower ball speed) test results 80

A.1 Bill of materials for ultrasonic system 92
A.2 Outdoor test results (2nd custom results omitted for neatness) 94

Chapter 1

Introduction

1.1 Background and Motivation

RADAR, having developed primarily during World War 2 for target detection and range determination has now grown into an extensive field with a wide range of applications from military and space applications to commercial products and recreational use. Modern RADAR systems, consisting of complex electronic and signal processing elements that are able to detect, track, identify, image and classify targets all whilst reducing interference from the environment [1].

Commercially, RADAR has been one of the variety of technologies used to assist in sports training and practice [2] [3] [4]. By using various technologies to measure velocity, sports performance can be measured and increased [5]. Often either RADAR, high speed video, laser or IMU (inertial measurement units) technology is used to detect velocity of objects in sport, with RADAR and video being the most common [3]. Increasingly as the use of technology in sporting applications has grown, so too has the use of new and improved methods for measuring and improving performance whilst training. Various devices are now used to track heart beat, step count, speed and position of a sports person.

Increasingly in ball sports, devices are used to measure ball velocity for training

purposes such as the PocketRadar [2]. Whilst larger more complex systems like Hawk-Eye, involving several high speed cameras to track ball data and speed exist, these are unsuitable for individual training sessions. Hence RADAR, specifically Doppler RADAR is commonly used due to its ability to track high speed projectiles over long ranges with a low degree of error, its immunity to lighting conditions unlike visual and infrared sensors [6] and its small and lightweight nature.

Doppler RADARs are based off the principle of the Doppler Shift in which, as shown below in 1.1, as an electromagnetic wave it is transmitted and reflected off of a moving object, its frequency changes in proportion to the object's velocity. By measuring the frequency shift of the received wave, one can determine the ball's velocity. Such systems tend to be expensive due to Doppler RADARs typically operating in the K band range at high frequencies (24 GHz), with specific components and signal processing algorithms implemented in a small compact manner. Furthermore, RADAR systems tend to be costly thus making it difficult to gain practical research with RADAR in academia. A possible solution to this price and accessibility issue, is an ultrasonic Doppler RADAR device to measure the velocity of sporting objects and to be used for RADAR demonstration purposes.

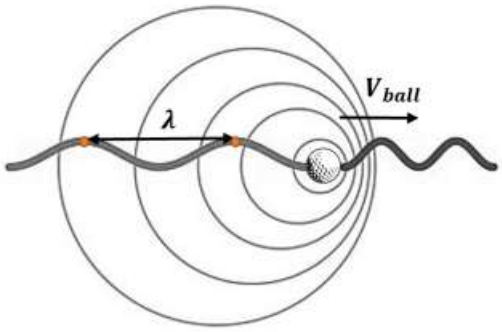

Figure 1.1: An illustration of the interaction between a moving object and an EM wave [7]

This research project focuses on a low budget hardware design and the initial signal processing design to allow for sports object tracking, and how the system may be used for RADAR demonstration purposes. The performance of the ultrasonic radar

is characterized and compared to that of an audio RADAR system as well as that of the S-Band coffee can RADAR system. The research project begins with outlining the main ideas and objectives behind the research, followed by a review of existing literature in ultrasonic radars and sports ball tracking, thereafter the methodology of the investigation is outlined, followed by the details of the design, results and conclusions.

1.2 Problem Statement

Major challenges with a demonstrator CW Doppler RADAR for sports tracking include:

- Accurately measuring high velocity objects with a narrow band ultrasonic transducer
- Accurately computing instantaneous velocity of balls found at varying ranges, from signals buried in noise
- Developing useful models and methods to practically characterize the performance of the ultrasonic system
- Ensuring a low-noise low-budget and robustly packaged RADAR system that can be expanded upon in later iterations

In attempting to solve these challenges outlined above, various RADAR literature was consulted that provided the following solutions:

- In [6] a threshold is chosen to filter out noise, and smoothing is performed on data to remove speckling in the spectrogram that can influence instantaneous velocity measurements. Furthermore, [8] provides insight into optimizing this threshold by iteratively carrying out various tests at varying ranges calibrating the threshold value. Lastly, spectrogram smoothing can be done to remove spikes of high power noise i.e. reducing the speckled nature of the spectrogram.

- In [6] distances of a few metres were achieved with ultrasonic sensors and in [8], it was suggested one can transmit at slightly below the resonant frequency of the transducer purposefully such that the received signal has greater bandwidth available to it, if one only measures incoming objects in which a positive doppler shift is expected.

- [9] and [7] provide good analytical approaches to characterizing performance of RADARs with propagating error and comparing performance of various systems.

- In [6] and [10] low budget ultrasonic systems were proposed from which the clipping, clamping and band-pass filter circuitry could be adapted. The remaining challenge is that of a reliable enclosure and power supply.

With most RADAR devices in sports applications operating typically in the GHz region at K band, there is a gap in the literature regarding the development of ultrasonic RADARs to accomplish a similar purpose at outdoor training sessions or indoor sporting events at much lower cost. The audio RADAR operates at lower frequencies of between 5 kHz and 15 kHz and thus could pose advantages with reduced circuit complexity. Furthermore, low-cost ultrasonic and audio systems can be used as demonstrator devices for RADAR for research purposes. This study serves to investigate and provide a proof of concept of an ultrasonic radar for estimating the speed of a high velocity object for sports applications specifically in tennis, cricket and football.

1.3 Objectives

The broad objective of this research project is to develop an ultrasonic radar system to measure an object's speed for sports training and entertainment purposes. The maximum, average and instantaneous velocity of basket balls, soccer balls, cricket balls and even squash balls will be determined and displayed. Customization of controls and display will be possible via GUI. A working PC-based implementation with a well packaged Veroboard-based hardware will be used. Ideally, a standalone

device would be developed which could sit beside a tennis net, behind a cricket net, behind a soccer net, next to a squash court's sidewall, and display the velocity of a ball passing in the vicinity.
The project includes the following objectives:

- Working hardware design implemented on Veroboard
- Signal processing to transmit and receive CW 40 kHz signal, and produce spectrogram plots, velocity over time plots and max and average velocity values for thrown object.
- GUI for changing parameters such as recording time, and for developers, various spectrogram parameters and sampling rate.
- Optimise pre-processing parameter values (ie. Parameter values needed to compute the spectrogram) and parameter values for algorithms needed to estimate the speed of the moving object.
- Comparison between performance of ultrasonic radar system versus acoustic SONAR system (microphone and speaker).
- Characterise performance of both the audio radar and the ultrasonic radar systems.
- Accuracy in estimating the speed of moving objects.
- Determining the operating range of the systems (ie how far must the ball be away for the system to produce reliable results).
- If time permits – packaging of the ultrasonic radar system (see diagram below).
- If time permits – produce PCB standalone version of system.

1.4 Thesis Contributions

The main contributions of this thesis are as follows:

- The design and implementation of a low budget ultrasonic system as an alternative to a K band Doppler RADAR is proposed.
- Characterising the performance of the ultrasonic system with various balls and environments (indoor and outdoor).
- Comparison between an ultrasonic, audio and RF-based radar systems for sporting applications.
- The system will be a demonstrator for RADAR concepts for research purposes.
- The project allows space to be iterated upon, going from a PC based system to a standalone well-packaged system.

1.5 Requirements and testing procedures

1.5.1 User Requirements

The general user requirement is to design and build an ultrasonic radar device to track and display the velocity of balls thrown in the device's vicinity, for sports training and entertainment. The device would be a demonstrator for RADAR for educational and research purposes.

Table 1.1: Table of User Requirements

Requirement number	**Requirement description**
R.001	The system shall estimate the speed of objects thrown in vicinity of device within suitable distance (either at device behind net, or past device)
R.002	The system shall display the estimated speed of objects on personal computer.
R.003	The system shall be a well-packaged device for indoor and outdoor use.
R.004	The system shall use ultrasonic or audio waves to measure a moving object's speed.
R.005	Device must be PC-based.
R.006	Device should be low cost and easy to setup – GUI to customize parameters.
R.007	Calculate speed of objects to a reasonable degree of accuracy.
R.008	Device must be easily powered out in the field, by a power bank or batteries or something else highly portable.

1.5.2 Technical Specifications

Table 1.2: Table of Technical Specifications

Requirement number	**Technical Specification Number**	**Technical Specification**
R.001	T.001	Ideally objects within 6 meters of radar are detected.
R.002	T.002	Speed is displayed on MATLAB initially. If time permits, make standalone device that displays speed.
R.003	T.003	Device needs to have a robust enclosure for indoor and outdoor use.
R.004	T.004	Continuous wave monostatic radar using ultrasonic frequencies – likely 40 kHz
R.005	T.005	Laptop will be used for generating and processing signals.
R.006	T.006	Matlab GUI developed and "plug 'n play".
R.007	T.007	With accuracy dropping off with distance, ideally an accuracy of +- 8km/h at 6 metres (existing baseball trainers)
R.008	T.008	Ultrasonic device must be powered from a 12V or 5V supply outputting a minimum of 100 mA. A Dual rail supply is needed to power the filter circuitry.

1.5.3 Acceptance Test Procedures (ATPs)

Table 1.3: Table of Acceptance Test Procedures (ATPs)

Technical specification	**Acceptance Test**	**Description**
T.001	ATP001	Conduct range test, measuring accuracy as one moves further from device up to 6 metres. Reasonable accuracy at 6 metres.
T.002	ATP002	Object is thrown in vicinity of device, speed is displayed thereafter on MATLAB GUI.
T.003	ATP003	Solid enclosure that meets user standards.
T.004	ATP004	Successfully transmit and receive ultrasonic frequency waves continuously in a room and outdoor space.
T.005	ATP005	Final device can be connected and run off laptop.
T.006	ATP006	Another user can successfully use device without difficulty.
T.007	ATP007	Measure speed of objects thrown at various distances from RADAR up to 6 metres.
T.008	ATP008	Power supply circuitry must produce +-12V rails from a single 12V external source i.e. a power bank.

1.6 Scope and Limitations

The major scope of the project is defined as a well packaged low budget hardware system for an ultrasonic CW Doppler RADAR with initial signal processing algorithms developed. The system needs to be developed and tested over a 12 week period from 2 August 2021 to 8 November 2021, As a result, the full scope is defined as follows:

- A highly portable 40 kHz CW Doppler RADAR for object tracking.
- Strip-board circuitry to allow for transmitting and receiving from a microcontroller. A PCB version is not part of the scope.
- Signal processing to extract and display instantaneous velocity, average velocity and max velocity values.
- Modularity to allow for future iterations and upgrades.
- Basic MATLAB GUI for user interaction with system.
- Comparison between Audio SONAR system and ultrasonic system as well as S-Band Coffee Can RADAR system.

1.7 Thesis Outline

The remainder of this thesis is organized as follows:
Chapter 2, Background: Background and literature review
Chapter 3, Methodology: Project methodology
Chapter 4, Design: Design and development
Chapter 5, Results: Experimental results
Chapter 6, Conclusions: Conclusions and future work

Chapter 2

Literature Review

- History of RADAR
- Fundamentals of RADAR
- The Doppler effect and Doppler RADAR
- RADAR versus SONAR
- Existing applications of ultrasonic system
- Existing Sports tracking-velocity Devices
- Characterizing the performance of a RADAR system

The literature review starts with a broad discussion on the history of RADAR followed by the fundamental principles of RADAR, various RADAR types and the differences between RADAR and SONAR systems before narrowing down to existing sports tracking velocity devices and a discussion on how to characterize the performance of a RADAR sports monitoring device.

2.1 History of RADAR

RADAR is an acronym for "radio detection and ranging" - first coined during World War 2 by the US Navy. RADAR theory was initially developed by Heinrich Hertz

in the 19th century, after proving Maxwells theory on electromagnetic radiation, but never practically applied until a German inventor by the name of Christian Hulsmeyer patented and invented a ship detection device to assist in collision avoidance [9]. The significance of the technology was not largely recognized until the 1930s when large military bombers emerged - this created a need for an early warning system [9]. Thus, in the 1930's, various RADAR systems were developed independently by several countries simultaneously. Early RADAR technology is argued as essential in "lifting the fog of war" and assisting in the Allies' victory in World War 2. Examples of initial RADAR's include the British Chain Home RADAR which provided early warning of German bombers during the "Battle of Britain" [11] and the American SCR-270 early warning RADAR [12].

After the war, RADAR continued to develop with implementations in broader areas including sports. Key steps in RADAR lending itself to sports usage include the invention of Doppler RADAR, its application to a speed gun for traffic fines, its application in baseball [13] and eventually the "Speed Gun" and "SpeedBall" invented by Henri Johnson [14]. Today various RADAR devices are used in sports to track baseball pitching, football shooting, golf club swings.

2.2 Fundamentals of RADAR

A RADAR system typically involves an electronic system emitting radio frequency (RF) electromagnetic (EM) waves (3 MHz to 300 GHz) towards a target and receiving the echoes that are reflected back from targets in that region. Using the characteristics of EM phenomena, one can calculate various values such as range and velocity. Basic RADAR systems consist of a transmitter, antenna, receiver and signal processor. See figure 2.1 below for the basic components of a RADAR system. When EM waves reach targets, currents are induced on the target and the target re-radiates the currents into the environment. Besides the target radiating some echoes back to the receiver, the wave emitted gets echoed back by other things in the environment as well - these unwanted signals are termed "clutter". The receiver thus "captures" a portion of a signal echoed from a target of interest as well as various

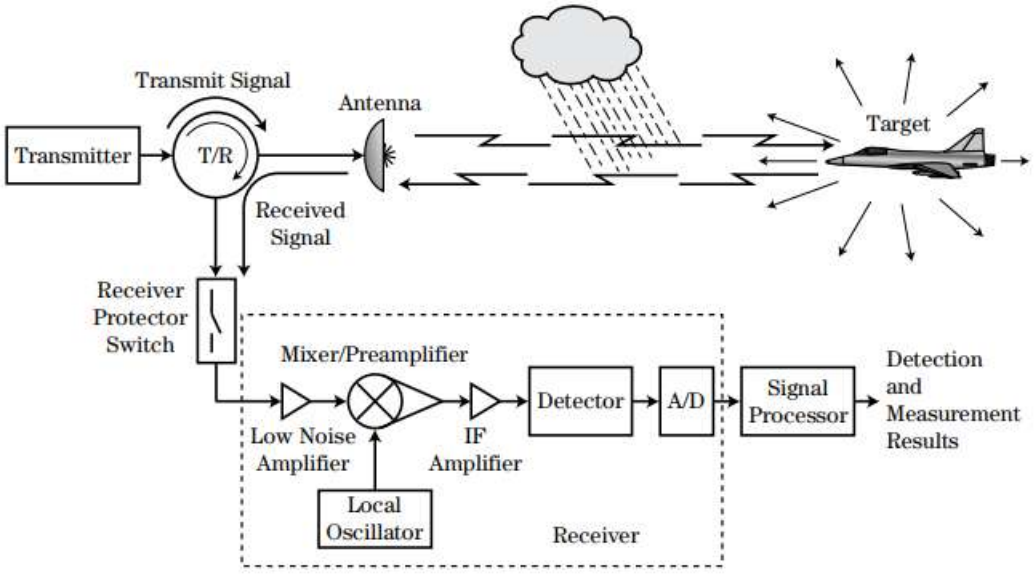

Figure 2.1: Basic RADAR system [1]

clutter from the environment. The receiver circuit functions to then amplify this weaker received signal, apply any filtering stages and then perform analog-to-digital conversion (ADC) to digitize the waveform from a continuous signal to a discrete representation, before being processed by the signal processor.

With the receiver being tailored to detect and receive low power signals, it is important to isolate it from the high powered signal being transmitted directly from the transmitter circuitry that could damage the receiver circuitry.
Two basic RADAR system antenna configurations include:

- Monostatic RADARs
- Bistatic RADARs

Monostatic configurations include one antenna that is used by the transmitter and receiver whereas in bistatic configurations, separate antennas are used for transmitting and receiving respectfully. However, this is not the only determining factor for

a monostatic or bistatic configuration. If the antennas are close together, perhaps even on the same device or structure, then the system is considered monostatic. If there is sufficient distance between the transmitter and receiver, the system is considered bistatic, i.e. the angles to a specific target should be sufficiently different. As mentioned previously, in a monostatic configuration it becomes vital to isolate the receiver from the transmitter.

In general there are three main types of RADAR used in object tracking:

- Pulsed Radar
- Frequency Modulated Continuous Wave (FMCW) RADAR
- Continuous-wave (CW) Radar

Pulsed Radars emit EM waves during short duration with a defined pulse width τ. During this time, the receiver is isolated from the antenna and thus protected but does not receive any EM waves from the environment. In the time between transmitted pulses of width τ, the transmitter is disconnected from the antenna and the receiver is connected and thus receives reflections of EM waves from the environment. The "listening" time together with τ represents a full pulsed radar cycle, called the interpulse period (IPP) or pulse repetition interval (PRI).

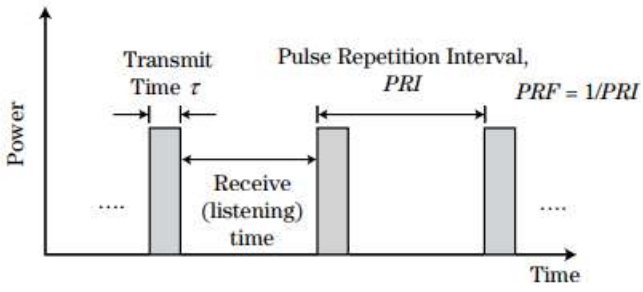

Figure 2.2: Pulsed Radar waveform [1]

By emitting a pulse and using the delayed echo, one can calculate the range to targets. With range and time information, velocity of the object can be derived and

plotted on a Range Doppler map [6].

FMCW Radars involve continuously transmitting frequency modulated signals in order to determine range and velocity of objects in the environment. By modulating the wave in frequency, a "timing mark" is put on the wave allowing for range determination. Differences in the transmitted and received echo frequency is known as the beat frequency - this can be used to determine target range and thus velocity [6].

CW Radars are typically much simpler systems that transmit a constant frequency waveform continuously. The velocity of a target can be measured using the change in frequency of the received echo. This theory is based on the Doppler effect. It is worth noting, that with CW radar only target velocity can be measured as there are no time marks able to be used to determine range. Furthermore, one can only measure radial velocity with CW Radars in a monostatic configuration as discussed later in the Doppler section. As a result of its simplicity, it is less computationally intensive. CW Radars are typically used in police speed-timing radars and altimeters and are typically limited to short range applications. [[1]].

2.3 The Doppler effect and Doppler Radar

Doppler Radars use the principle of the Doppler effect where interactions between electromagnetic waves and moving objects produces a frequency shift that is directly proportional to the velocity of the object.

With a moving scatterer or object, the received frequency is described as follows [1]:

$$f_r = (\frac{1 + \frac{v}{c}}{1 - \frac{v}{c}})f \tag{2.1}$$

As shown in (2.1) above, an approaching target will cause an increase in received frequency and vice versa. This is extremely useful in separating high power clutter echoes from a target's echo - stationary clutter will not experience a frequency shift while a moving target will. Figure 2.3 below illustrates the Doppler effect.

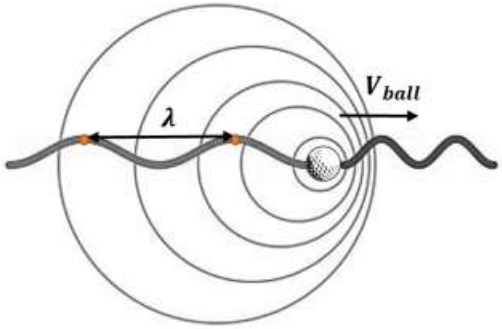

Figure 2.3: An illustration of the interaction between a moving object and an EM wave [7]

Equation 2.1 can be simplified into the following form [1]:

$$f_r = [1 + 2(\frac{v}{c})]f \tag{2.2}$$

The received EM wave frequency can thus be expressed as a combination of the transmitted wave's frequency and the experienced Doppler shift:

$$f_r = f + f_d \tag{2.3}$$

where, noting $c = f\lambda$, f_d is then:

$$f_d = \frac{2v}{c}f = \frac{2v}{\lambda} \tag{2.4}$$

Thus by measuring the Doppler shift of a received waveform, one can determine the radial velocity of the object it interacted with. For a monostatic CW radar configuration, one is measuring the Doppler shift that is proportional to the target's velocity along the line of sight (LOS) of the target and radar system. Velocities not directly toward or away from the RADAR cannot be measured i.e. only radial velocities are measured. Thus if the angle between the LOS and object's velocity vector is not zero, the doppler shift becomes:

$$f_d = \frac{2v}{\lambda}cos(\phi) \tag{2.5}$$

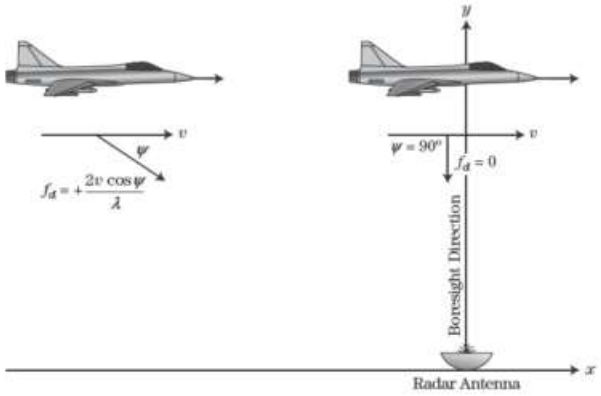

Figure 2.4: An illustration of the Doppler shift and how it relates to the radial component of a target's velocity [1]

Doppler resolution is an important consideration when creating a Doppler radar. Doppler resolution is the minimum difference in Doppler shifts of two received signals from two targets at which they can be reliably distinguished before blurring together. By increasing the Coherent Processing Interval (CPI) one can make the Doppler resolution finer.

When attempting to visualize the Doppler frequency of a received signal, a spectrogram is often used. A spectrogram consists of a series of overlapping Short Time Fourier Transforms plotted as a function of time and frequency. One can thus visualize Doppler shifts against time, with a colour map showing the density or value of the STFT in the matrix relative to other values. Spectrograms are often used to analyse Doppler RADAR data and will be a useful tool in this investigation.

2.4 RADAR versus SONAR

SONAR is an acronym for Sound navigation and ranging and is similar in principle to RADAR in terms of transmitting a wave into the environment and measuring range and velocity of objects based on the returned echo. The difference therein lies with SONAR transmitting sound waves (mechanical wave) instead of EM waves. Thus the speed of propagation for sound waves is $c = 343\ m/s$ whereas the speed of

EM waves is $c = 3x10^8\ m/s$. EM waves do not require a propagation medium where as sound waves propagate through mediums like air or water through vibrations.

The speed of sound waves depend on the air temperature, pressure, density and gas composition. If one of these factors changes, error can occur in the measurements. As a result, ultrasonic sensors are rather better suited to simple measurements with more constant conditions [15]. Thus ultrasonic RADARs can be less reliable and accurate than high frequency RADARs due to sound waves being affected by changing environments and propagation mediums but such sensors do offer a cost effective method of measurement and object tracking.

When creating a Doppler SONAR system, ultrasonic frequencies are preferable over lower frequency audible SONAR due to ultrasonic SONAR being inaudible and less background noise existing at that frequency [6]. Similar to RADAR methods, CW Sonar and Pulsed Sonar methods are often used for object detection [6]. FMCW Sonar is not often used as a result of the challenge of modulating frequency within a narrow bandwidth. Micro-Doppler signatures, being smaller Doppler reflections from movements on the surface of the target relative to the target can be used to measure spin and other characteristics of sports balls.

In terms of ultrasonic radar hardware versus RADAR hardware, there is little difference. Both technologies make use of transmitters and receivers and various signal processing elements. As mentioned previously, the difference lies in the wave being transmitted. Thus ultrasonic transducers differ in that they vibrate a membrane or medium in order to produce ultrasonic waves and are typically available at an operating frequency of 40 kHz with a narrow bandwidth of 2-4 kHz. Ultrasonic transducers rely on the Piezoelectric Effect in which a material expands or compresses in response to a voltage applied. Such materials can be frequency dependant and thus resonant at specific frequencies. Thus, if one applies a periodic voltage one can propagate a pressure wave through a medium in the form of ultrasound. Conversely, the pressure wave can be received as a voltage signal [10].

In terms of important equations for RADAR, the total power received at a receiver after a signal is transmitted and reflected back can be expressed as follows [11]:

$$P_r = \frac{P_t G_t}{4\pi R^2} \frac{\sigma A_e}{4\pi R^2} \tag{2.6}$$

where P_r is power received, P_t is the peak transmitter power, R is the distance from the distance from the radar, σ or RCS is a measure of energy a target intercepts and scatters back towards the receiver [11] measured in m^2. G_t is the transmit gain, and A_e is the effective area of the receiving antenna. It is worth noting for this investigation, that the received power, P_r, is directly proportional to the RCS of the target, and exponentially indirectly proportional to the distance to the target.

2.5 Important signal processing concepts

- Nyquist Criterion
  This concept states that the sampling frequency should be at least twice the highest frequency to be obtained in the spectrum: $f_s > 2f_N$. Thus to correctly sample a 40 kHz signal without aliasing, a sampling frequency greater than 80 kHz is required.

- Frequency resolution:
  This is the difference in frequency between each frequency bin which thus limits precision. It can be calculated as $\frac{SamplingFrequency}{DFTsize}$.

- Windowing:
  This is an important concept which involves applying a limited non-zero length function to a signal that helps reduce the sidelobes of a signal in the frequency domain. Examples of window functions include a hamming window and Hann window and Nutall window and Blackman window.

- Baseband shifting:
  A time domain signal can be shifted down in frequency by applying a complex exponential to it. By applying an exponential at the centre frequency, f_0, one gets a complex signal of IQ data that can provide a baseband version of the

original spectrum - i.e. a 40 kHz original signal is now centred about the origin instead of 40 kHz.

- Signal to Noise ratio:
  SNR is a measure of signal power compared to noise power in a spectrum. The higher the SNR, the stronger the signal is with respect to noise, and the easier it is to detect when buried in noise. It can be given by:

$$\frac{S}{N} = \frac{|v_o(t_{peak}|^2}{|n_0|^2} = \frac{E}{\frac{\eta}{2}} \tag{2.7}$$

2.6 Existing applications of ultrasonic systems

Ultrasonic technology has been used in a variety of applications such as biomedical technology, gesture recognition and sensing, 3D imaging and indoor mapping, echo ranging with SONAR, Flaw Detection with Non-destructive Testing methods (NDT), tracking, active safety systems and level monitoring in industrial automation.

2.6.1 Ultrasound in medicine

Ultrasound technology is used extensively in medicine for examinations such as abdominal, cardiac and maternity examination [16]. Ultrasonography is an ultrasonic imaging technique that visualizes subcutaneous soft tissue body parts like tendons, muscles, vessels, internal organs and joints. A hand-held probe (transducer) is placed on and moved over the patient with a gel used to couple the ultrasound between the transducer and patient [16]. There are four modes of ultrasound medical imaging:

- A-mode: Simplest type of ultrasound in which a single transducer scans a line and plots echoes as a function of depth.
- B-mode: This mode uses a linear array of ultrasonic transducers simultaneously scanning a location and producing a two-dimensional image.
- M-mode: This motion-mode involves a sequence of B-mode scans being taken to see ranges of motion.

- Doppler mode: The Doppler effect is used in measuring blood flow. Blood is measured as either moving away from or towards a probe by measuring the radial velocity of blood. This is often used in cardiovascular studies and determining portal hypertension [16].

For more details on ultrasound applications in medicine see [16].

2.6.2 Ultrasound in Deep learning and gesture recognition

Ultrasonic applications in Human Computer Interactions (HCI) namely gesture recognition have also been explored such as by C. Lin in [6]. In Lin's dissertation, a Doppler SONAR system was created, with three receivers, to sense Doppler frequency shifts of hand gestures and use the received data as inputs to two deep learning models - a Long-Short Term Memory (LSTM) network and a Convolutional Neural Network (CNN). The models were trained to be able to classify hand gestures made in front of the ultrasonic transducers. The study showed it was possible to classify six basic gestures with reasonable degree of accuracy, and that SONAR could be applied in similar areas that RADAR is currently being used in - such as deep learning techniques. The study further shed light on SONAR transmitter and receiver circuitry design, a data logging service and signal processing techniques commonly used for Doppler radars. Lin goes into detail with useful analog circuitry calculations such as slew rate, gain bandwidth product, cutoff frequencies and bandwidth that determines component choice as well as the type of filters used. Limitations found in this dissertation included the use of a Butterworth Low Pass Filter (LPF) in the reconstruction filter in the transmission circuit - the component provided is both expensive and requires a clock. As a result, other component choices in this regard were considered instead.

2.6.3 Ultrasound in driving-aid and active safety systems

Ultrasonic sensors are proposed for their use in active safety systems in [8] specifically for Adaptive Cruise Control (ACC). In this study, an ultrasonic ACC prototype is developed for low speed and short distances. The ultrasonic system was proposed

for its cheaper, less complex and less computationally intensive nature. The system was shown to be effective in detecting obstacles and carrying out responsive actions on the accelerator and brakes via a designed control system and comparing values to a known safety distance threshold. It was concluded that coupling such a cheaper alternative to radar or computer vision solutions with other sensors could allow ACC to be implemented in lower-end vehicles. Apart from advantages, the study explores the disadvantages of ultrasonic sensors such as the narrow bandwidth thereof, short range due to attenuation of ultrasound in mediums like air and low response time due to low propagation speed relative to RADAR. The study explores useful error analysis such as the detection of false echoes produced by road turbulence when the threshold is too low in the signal processing and similarly no response from the control system when the threshold is too high. The final threshold was determined by carrying out a series of echoes over a specified range and measuring at what threshold a false echo is detected.

2.6.4 Ultrasound for indoor mapping

A paper by Antonio Tedeschi in [17] explores the use of an ultrasonic RADAR system for blind mapping of indoor environments and displaying information to an android-based device. In the system HC-SR04 and HC-SR05 ultrasonic sensors are used to transmit and receive a series of ultrasonic pulses at 40 kHz in order to measure the distance to an object from the sensor, if it is within the sensor's range (2cm to 400 cm). Data is measured and processed by an Arduino Nano and distance measurements are sent to an android device via a Bluetooth module. An android application serves up the information to the user as a depiction of what obstacles are nearby. Similarly a Virtual Reality view was developed to be viewed via Google Cardboard. The system was developed as an inexpensive alternative to sensors such as an RGB camera, and showed other advantages such as the compact nature and light-free mapping capability of the Ultrasound Radar System (URAS).

2.6.5 Ultrasound for level measurement and industrial applications

Ultrasonic sensors are often used for detecting a range of materials for tasks such as material handling, fill level measurement or detection of gates and doorways. Ultrasonic sensors can be used to detect most materials like milk, chemicals, lacquer or mud. The fill level of silos and tanks used in dairies, chemical plants and mineral companies can be thus monitored. This is useful in situations such as open-cast mines which excavates large amounts of materials like sand, rock and gravel that must be stored until the material can be transported away from site. Ultrasonic sensors are used to determine when the maximum fill level in a gravel silo has been reached. Furthermore, ultrasonic sensors are often used in waste water treatment plants (WWTPs) to monitor and prevent overfilling of containers storing sewage sludge [18].

Apart from level measurement, ultrasonic sensors are used in agriculture for optimizing spray coverage over uneven terrain or changing crop heights. Measurements allow the height of the spray boom to be monitored and adjusted whilst being immune to dust, dirt or chemicals in the region of interest. Furthermore, when spraying pesticides on trees, ultrasonic sensors are used to detect gaps in the tree and stop the spraying process so that pesticides do not get within the gap of the tree and damage it.

Ultrasonic sensors are also used in anti-collision detection for aerial work platforms, often used on construction sites. They are also used in parking garages to detect the presence of a vehicle underneath a barrier so that the barrier is not lowered when the vehicle is present. There are many more applications of ultrasonic sensors in industrial automation scenarios mentioned in [18].

2.7 Existing Sports tracking-velocity Devices

2.7.1 Types of sensors used in various sports applications

Technology has been increasingly used in sports for enhancing performance, as technology has reduced in cost, increased in availability and advancements in wearable technology have occurred. As the Internet of Things has grown, it has entered sporting applications with devices being used to track heart rate, pulse count, positional and movement data, temperature data, and speed. Some devices used in sports now include Sony's Smart Tennis Sensor, Addidas miCoach Smart ball, wearable technology like FitBit, Nike Fuelband, Garmin's Vivofit and PocketRadars. Various wearable devices now commonly incorporate various sensors such as pedometers, accelerometers and gyroscopes, GPS sensors and physiologic sensors (heart rate monitors, temperature monitors and integrated sensors). With such sensors, sportsmen and sportswomen can log their heart rate, temperature, speed, steps, distance and energy expenditure and thus quantify their training and exercise [19].

Incorporating sensors into sports equipment allows for example baseball players to measure the speed and force with which they hit a baseball, or how fast a golf club is swung (such as in Cobra Connect [20]), sensors in helmets in high contact sports measure impact and give data regarding concussions, starting blocks in athletics or swimming detect false starts, player statistics can be measured and displayed to audiences and eCoach devices can help people correct posture, golf club swing or training intensity [20].

Sensors specifically used in velocity tracking of sports balls commonly include laser or IR sensors, Inertial Measurement Unit (IMU) devices, high speed video recording and microwave Doppler radar modules (microwave sensors) [3]. Laser and RADAR systems work similarly to one another in which the Doppler effect is used to estimate the speed of an object and the distance away from the device. Lasers do the same, usually with more precision and information. Both systems are typically statically placed and mounted on a tripod, with nothing obscuring the region in front of them.

IMUs estimate measurements with assumptions based on the movement performed such as a common swing of a bat - this has obvious issues if one's swing style varies [3]. Accelerometers calculate the estimated result of wrist or arm speed and are thus less suitable for ball speed measurement. Conventional cameras are used sometimes but for simple measures of velocity - RADARs are typically used for balls because of their instant feedback, simplicity and cost depending on the application. Thus the specific application of tracking velocity will require varying devices be it laser, RADAR or IMUs. Another system commonly used for ball velocity tracking is the Hawk eye technology in cricket. Hawk-Eye (shown in 2.5) is a computer vision system that uses six cameras around an area that collects data on a moving balls [21]. It identifies an image of the ball in each frame and calculates the ball's position by comparing its position to other separated cameras at that time instant. Successive frames build up a record of the ball's path followed and from this and the camera speed and time between frames, velocity can be calculated. Whilst this system is accurate it is not suitable for an individual with limited funds.
As a result one can look specifically at laser, IR and radar sensors for ball tracking for a low cost option. In [23] it is shown that ultrasonic sensors are not able to efficiently detect fast moving objects when compared with laser sensors which had very high accuracy. However this study lacked a greater depth of investigation into the performance of the ultrasonic sensors.

IR LEDs emit EM waves in the infrared region with a peak wavelength of 940 nm. With low forward voltage and 20 mA of current, it is flexible to be used with most supplies. Laser diodes on the other hand operate with a wavelength of 650 nm, outputting 5mW and being driven from 2.8 to 5.2 V. Laser sensors tend to operate over a larger distance than IR sensors but are highly directional in nature compared to IR sensors. Both types of sensors are relatively accurate and can operate in real-time however are not very robust and delay can be experienced over large distances [23].

An example of a microwave sensor is the HB100 X-Band transceiver operating at 10.525 GHz. It can be powered with a +5V duty cycle to limit power consumption. The performance of the Doppler radar is dependant on the amplification circuit and

Figure 2.5: Hawk-Eye system and its cameras in a stadium [22]

signal processing, but such modules are able to determine the velocity of objects accurately by means of the Doppler shift frequencies measured. Possible disadvantages include receiving nearby noise and frequencies that interfere with results [23] as well as typically higher cost than ultrasonic sensors. Other examples of commonly used sports Doppler RADARs include Arrowspeed Radarchron, Break Speed Radar and Swing Speed Radar [24].

Ultrasonic SONAR sensors offer the advantage of being inexpensive and highly robust whilst being immune to weather changes and lighting conditions, but suffer from typically narrow bandwidths which would limit the maximum Doppler shifts detected. Acoustic SONAR offers similar benefits, but its audible nature is not ideal for a sports application.

2.7.2 Application of RADAR in sports

Doppler radar is used in sports such as golf, baseball, tennis and cricket involving projectile motion [7]. Examples of existing Doppler Radar products include Trackman, FlightScope, PocketRadar (see 2.6), Net Playz multisport radar and Stalker sports radar products [4].

Figure 2.6: Compact PocketRadar device used to measure ball speed [2]

An evaluation of Doppler radar in sports applications is done by Martin in [9] in which a Trackman II X radar device measures a baseball being hit. Similar to this investigation, Martin uses a continuous wave radar albeit X-band, not ultrasonic. This dissertation offers some insights to this investigation as it analyses baseball motion - similar to that of a cricket ball or tennis ball. Martin evaluates velocity and spin of a sports ball in his dissertation and offers insight into how performance of a radar system is analyzed.

The methodology includes using a high speed camera and a system of infrared cameras to have results to compare with the Doppler radar results. Martin then conducts a rigorous assessment of how the data is affected by noise, is filtered and the accuracy of the data.

This dissertation is limited in that it does not offer insights into the building and designing of a RADAR but rather the measuring and analysis of data from an existing radar device. It furthermore has wide spread repetitive results provided - which, whilst not being summarized well, adds to the in-depth nature of his analysis.

2.8 Characterizing the performance of a RADAR system

In Martin's dissertation on "Evaluation of Doppler radar ball tracking and its experimental uses", he compared results from a high speed camera filmed system to the radar system to determine accuracy. Distances over which tests were done were measured and kept constant. Furthermore the effect of multi-path reflections and noise was investigated by comparing the performance of balls hit at different angles to the pitcher line. Thus by varying the angled position of the RADAR as well as varying angles of the ball from the LOS of the RADAR, its performance was determined. A piece-wise derivative of position data over time could furthermore provide a velocity comparison to the velocity calculated with the Doppler shift from the RADAR data. Various repeated measurements were taken and averaged for all calculations to provide reliable data sets. Lastly, the root mean squared error is a useful statistic in order to evaluate average error in velocity versus time results from the RADAR.

Ideally in testing RADAR technology, repeatable conditions need to be possible with many tests being undertaken. This is not possible in an outdoor changing environment which necessitates the use of simulators which can return simulated data for an environment and object that a RADAR is trying to detect. Such Hardware in the Loop simulation can reduce costs, time to test a system and improve accuracy [7]. A Doppler simulator can be used for this purpose, but requires building one for ones use case.

2.9 Critical Review

In reviewing the literature of SONAR and RADAR applications and implementations, there seems to be a lack of investigations into the application of a portable ultrasonic radar to high velocity object tracking - specifically in sports scenarios. Whilst many Doppler sports RADAR guns and launch monitors exist, there seems to be little usage of CW ultrasonic radar approaches which can reduce costs and

device complexity.

Furthermore, whilst RADAR theory is important, often people miss out on useful hands-on experience with RADARS to truly grasp the concepts. With the high cost and complexity of RADAR systems it can be difficult for students and academics to experiment in this field [25].

Thus this project serves to address this gap in the literature by designing a well packaged ultrasonic radar demonstrator to reliably measure sporting objects for demonstration and research purposes. The project is focused on the hardware design and initial signal processing of the RADAR demonstrator so that the radial velocity of sports balls can be measured reliably.

Chapter 3

Methodology

3.1 Methodology Overview

The project followed an approach similar to that of an AGILE model with regular meetings with Dr Yunus Abdul Gaffar, regular testing in tandem with the development of the project and rapid development over a short period. The approach to the research project included the following key steps, which were organized into a Gantt Chart to guide the project, in order to develop a working ultrasonic CW RADAR sports tracking demonstrator:

- Theory Review and Learning Plan
- Literature Review
- Hardware Design
- Signal Processing Design
- Audio SONAR testing
- GUI Design
- Enclosure Design
- Ultrasonic RADAR testing

- Analysis of Results
- Conclusions

3.2 Project Phases

First the relevant concepts of general RADAR were covered to give background to the study, before delving deeper into CW Radar theory and appropriate signal processing concepts. Following this, a review of the appropriate theory was done and a specific scope of the project was defined and reviewed by Dr Yunus Abdul Gaffar. Once an adequate understanding of the problem and its scope was established, a review of relevant literature was done. This involved researching general RADAR literature and concepts before delving deeper into CW RADARs and thereafter, tunneling down into sports RADARs and sensors used in sports.

After a literature review was done, there was sufficient understanding to begin the hardware design, working with C Lin's [6] and Curry's [10] initial circuits to develop a final design. In tandem with this process, initial signal processing algorithms were developed in order to begin testing with an acoustic SONAR system. This was done so that a working signal processing algorithm could be ready for testing on the final ultrasonic system when completed.

After initial results were collected on the AUDIO Sonar system (using a microphone and speaker connected to a sound card), a basic GUI was designed for a user to interact with the system, which could be used for the ultrasonic system as well. Hereafter, whilst the ultrasonic hardware was being assembled and tested, an enclosure was designed for the ultrasonic system and 3D printed.

Following this, the ultrasonic hardware was integrated with the enclosure and signal processing program for testing. Experiments were planned and carried out. Results were collected and compared to that of the audio SONAR system, and using the results, the performance of the ultrasonic system and viability thereof was concluded.

3.3 Data collection and logging

Once the signal processing algorithm was implemented and tested on an audio SONAR system, results were collected and logged by means of the MATLAB GUI and a XONAR U5 Sound card. In the MATLAB GUI, a sampling time, sampling frequency, transmit frequency and spectrogram parameters are chosen, and thereafter, the received time domain samples are saved along with the centre frequency, sampling frequency.

Recorded data via the signal processing application was saved as a .mat file. When the experiments were carried out, there were many data sets obtained from which the max and average velocities need to be obtained. Thus a data extraction script was written to loop through all the .mat files in a chosen directory and process the data to obtain the velocity measurements and save these iteratively to an array. After all the data sets are processed, the velocity measurements stored in the array are saved to a .csv file along with the respective data set name for each measurement. The file naming convention for measured data sets are set as ¡Ball used¿_¡System¿_¡Distance¿. The required threshold value to separate noise from a signal of interest, was set using a calibration function which transmitted and received a signal five times in a static environment, took the max power of the noise in each case and obtained the mean thereof. The threshold was then set as 80% of this value.

3.4 Experiment Design

In the sport RADAR industry one can use Doppler Simulators to help test the system. However, due to the experimental novel nature of the design, measurements were taken out in the field in order to characterize the system's performance.
Tests specifically carried out to characterize the system included:

- Determining the ideal transmitting frequency for the audio and ultrasonic RADAR systems.
- Determining the noise threshold of the two systems.

- Determining the best velocity extraction algorithm.
- Determining the maximum range of the system.
- Determining the various sizes of balls the system can detect i.e. the minimum RCS necessary to be detected.

The tests were carried out on the ultrasonic system as well as the audio SONAR system and compared with that of an S-Band MIT Coffee Can RADAR system as well. All system's results were compared with calculated velocity value to ensure accuracy of results produced. This involved filming all experiments and having a tape measure to measure distances of the ball travelled. Using time stamps observable from the video and distance from the tape measure, one can determine a reliable average velocity value for each experiment to corroborate each experiment's produced velocity values. See the experiments further elaborated on below.

3.4.1 Ideal Transmit Frequency Experiment

In an indoor environment, a distance of 2.5 metres was measured. The audio and ultrasonic systems were aimed directly upwards and a tennis ball was dropped down towards the RADAR systems. The RADAR systems were setup to transmit at varying frequencies (8, 10, 12 and 14 kHz for audio RADAR and 38, 39, 39.5 and 40 kHz for ultrasonic RADAR). The associated velocity measurements and max SNR were recorded and compared. From the results, the ideal transmit frequency could be chosen of the audio and ultrasonic system's respectively.

3.4.2 Noise Threshold

The noise threshold was experimentally determined by collecting results in a static non-moving environment. The maximum amplitude of noise observed in the spectrum could then be used as the minimum threshold to observe signals. This test can be repeatedly carried out in a variety of environments to determine an optimal threshold value. A calibrate function was thus written to transmit and record in a static environment and return the maximum noise level in dB in the spectrum. This

was repeated 5 times and the average was returned. The value was then adjusted experimentally as needed to obtain the ideal value. In general, 90% of the calibrated value was used.

3.4.3 Algorithm Tests

A custom velocity extraction algorithm, with varying parameters, needs to be compared with that of a median frequency extraction algorithm, which can be compared to reliable true velocity measurements obtained from video recordings.

Using video measurements, one can produce velocity estimates. For the indoor experiments, one could determine the final velocity measurements using the change in time for the ball's flight as well as the change in distance and the acceleration due to gravity (9.81 m/s) as shown in 3.1:

$$r = r_0 + v_f t - \frac{1}{2}at^2 \tag{3.1}$$

where r is the object's final position,
r_0 is the object's initial position,
v_f is the objects final velocity,
t is the interval of time,
and a is the acceleration on the object, i.e. 9.81 m/s.

The average velocity could also be determined with $\frac{Distance}{Time}$. The change in time was recorded by stepping through the videos frame by frame and recording the moment the ball was released and caught. The distance was also measured and marked before hand.

Using a custom algorithm involving an STFT, smoothing, thresholding, removing values without neighbours and then extracting the max frequency in each frame and multiplying by a conversion factor, velocity estimates could be obtained. The parameters for the STFT were set as 2^{12} samples per frame and 90% frame overlap, and 2^10 samples per frame and 70% frame overlap in order to investigate further the

best parameters for the spectrogram.

Using the pspectrum and medfreq MATLAB functions, velocity estimates could be produced. The pspectrum returns a power spectrum matrix with which the medfreq function can return an array of frequencies which can be multiplied by a conversion factor to produce velocity estimates. A threshold of -80 dB was used and a frequency resolution of 128.

Uncertainties for all measurements were propagated, then each ball experiment was investigated by comparing the video, custom and medfreq velocity measurements with uncertainty. The percentage was then taken of how much the custom algorithm agreed with the video measurements, how much the medfreq algorithm agreed with video measurements and of how much the custom algorithm agreed with the medfreq algorithm. In this way, the best algorithm could be chosen.
The sources of uncertainty identified are listed below:

- Measuring distance markers (tape measure).
- Reading distance off video.
- Measuring time off video.
- Reading velocity from spectrogram.

3.4.4 RCS Tests

Various ball tests were carried out over varying distances and with balls of varying size. A basket ball, football, rugby ball, tennis ball and squash ball were used in experimentation i.e. reducing the RADAR Cross Section (RCS) of the object. By using the most accurate velocity extraction algorithm previously determined, the success rate per ball can be determined and thus the maximum size ball that can be detected.

3.4.5 Range Tests

The maximum range of the system was determined by cross referencing the spectrogram produced with the video, and observing when the ball is visible in the spectrum and where the ball is at that time frame in the video, with reference to the distance markers. In this way, the maximum distance and size of objects that the system can observe was recorded.

In the following section, the design of the ultrasonic hardware, signal processing and GUI is presented.

Chapter 4

Design

4.1 System Design Overview

The overall system consists of three subsystems:

- Hardware Design
- Signal Processing Design
- GUI and Data logging Design

A system overview is given below showing the system on a macro level:

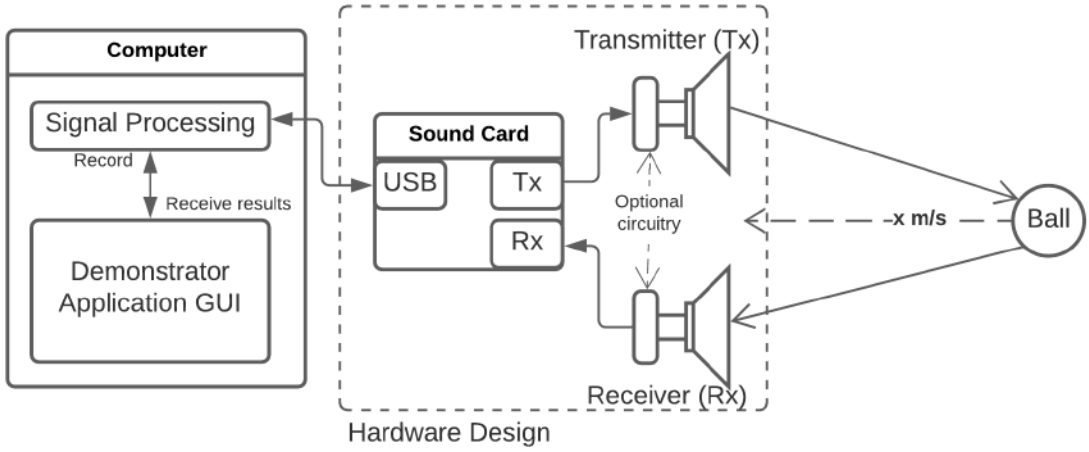

Figure 4.1: System overview showing the system's subsystems

The three subsystems mentioned are thus observable in the overview. Note that the "optional circuitry" is referencing the Tx and Rx circuits used for the ultrasonic system, but the audio system does not use any.

4.2 Hardware Design

Of the Hardware subsystem, 3 different subsystems were used to obtain results:

- Audio RADAR system
- Ultrasonic RADAR system
- S-Band MIT Coffee Can RADAR system

This section details the specific circuits and components used to build the ultrasonic system, as well as hardware used for the audio RADAR system and the S-Band RADAR system. The ultrasonic system consists of 3 main hardware components that being the power supply circuitry, transmitter (Tx) and receiver (Rx) circuitry. The audio RADAR and S-Band Coffee Can RADAR used previously-available equipment. These will be discussed in detail below along with the ADC/DAC used for all 3 systems.

4.2.1 Data acquisition Device - ADC/DAC

All 3 systems (ultrasonic system, audio RADAR and MIT Coffee Can RADAR) used a sound card as the DAQ with which a signal could be sampled. This ties in with the project scope being a PC-based ultrasonic RADAR demonstrator, thus time was not spent on using a microcontroller ADC/DAC.

A XONAR U5 sound card was used as the system's DAQ, with two AUX cables, with the following specifications:
The sound card sample rate was set to 192 kHz at a resolution 24 bits. This allows the system to sample signals at frequencies below 96 kHz without error, according to the Nyquist rate. The sound card is also configured to record mono channel and

Table 4.1: Table of sound card specifications

Parameter	**Specification**
SNR	104 dB
THD+N (total harmonic distortion plus noise)	0.005%
Frequency Response	<10 Hz to 44 kHz
Sample Rate and Resolution	Up to 192 KHz @ 16/24 bit
Bus Compatibility	USB Audio class 2.0 for all functions USB Audio class 1.0 for playback
Power Supply	USB-powered
Headphone amplifier (impedance)	32-150 ohm

not stereo. All configurations were done in MATLAB, whilst sound control panel settings needed to be altered to set the sample rate and bit depth to the higher 192 kHz and 24 bit.

4.2.2 MIT Coffee Can RADAR System

This project did not have access to this RADAR system, however results from a previous investigation were used by Andrew Bodenstein in [26]. The system is detailed below.
The system consisted of the following components:

- XONAR U5 Sound card as the ADC/DAC.
- 12V Lead acid Battery
- Filtering circuitry in the form of a PCB
- RF circuitry
- Coffee Can antennas

See an image of the system below:

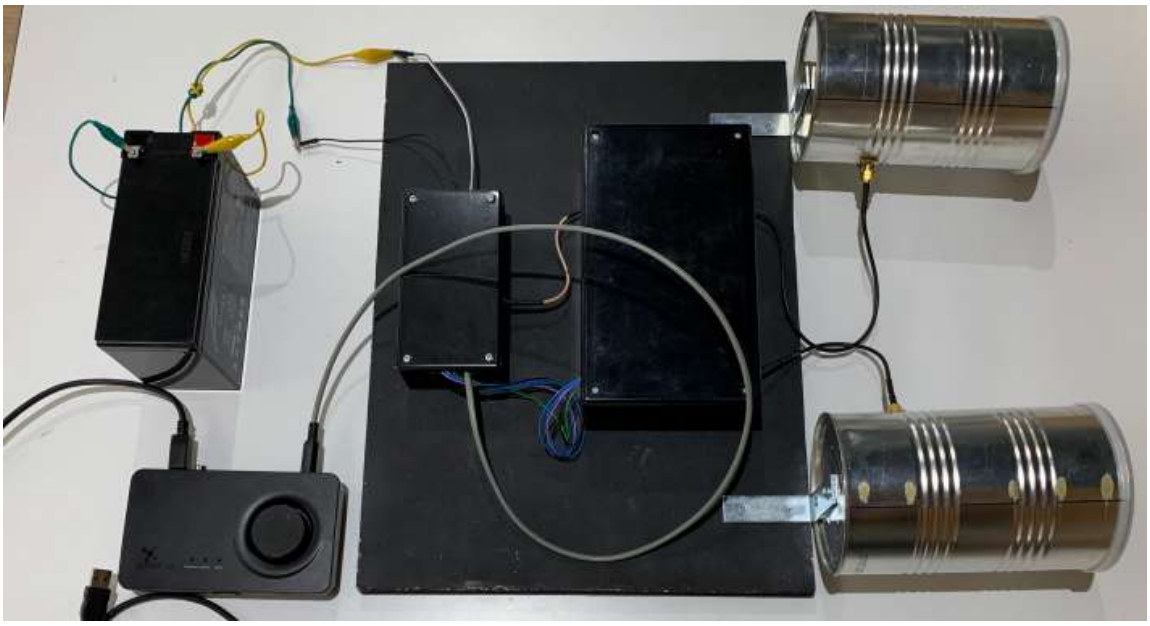

Figure 4.2: MIT Coffee Can RADAR system setup with the above components [26]

4.2.3 Audio RADAR System

The audio RADAR system consisted of a speaker and microphone with which an audio signal could be transmitted and received from respectively. Only a single channel is used when transmitting and receiving. The details of the hardware used are shown below:

Table 4.2: Table of Transmitter (SP-HF160 speakers) Specifications

Parameter	Specification
Output Power	4W (RMS)
SNR	80 dB
Speaker Drivers	4 Ω
Frequency Response	160 Hz - 18 KHz
Dimensions	83.5x128.5x84mm (WxHxD)

Figure 4.3: SP-HF160 speakers used as the transmitter in the audio RADAR system

Table 4.3: Table of Receiver (Havit HV-M80 microphone) Specifications

Parameter	Specification
Frequency response	30 Hz - 15 KHz
Impedance	¡ 10KΩ
Sensitivity	-58 dB
Wire length	1.5m
Plug	3.5 mm stero

Figure 4.4: Havit HV-M80 microphone used as the receiver in the audio RADAR system

4.2.4 Ultrasonic System Design

The four main subsystems of the ultrasonic system include the transmitter, receiver, power supply circuitry and enclosure. It is worth noting that the ultrasonic system design was done in such a way to remain modular and allow for future improvement. Circuitry and enclosures were designed to allow for the system to move away from a PC-based approach to a standalone system. See the complete Bill of Materials at A.1 in the Appendix. See the figure below for an overview of the ultrasonic system:

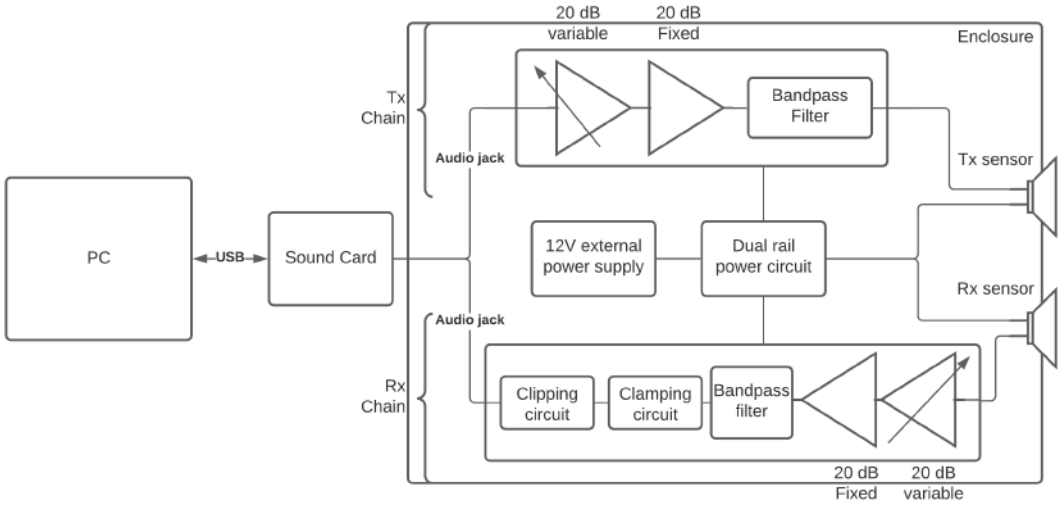

Figure 4.5: Overview of the design of the ultrasonic system

Ultrasonic Transducer selection

Options for ultrasonic transducers are fairly limited, with primarily ultrasonic barrel transmitters and ultrasonic microphones being available. Since a PCB was not being developed and thus no SMDs used, a PZT ultrasonic barrel transmitter and receiver was chosen, being readily available and operating outside of human hearing at 40 KHz. The specifications for the ultrasonic barrel transmitter and receiver are detailed below:

Table 4.4: Table of ultrasonic barrel transmitter specifications

Parameter	Specification
Centre Frequency f0	40 +- 0.1 kHz
Bandwidth (-6dB)	2 kHz
Directivity	80 degrees
Sound Pressure Level	120 dB @ 20 Vpp
Capacitance	2400 pF +- 20%
Impedance	400 ohm @ 40 kHz

Table 4.5: Table of ultrasonic barrel receiver specifications

Parameter	Specification
Centre Frequency f0	40 +- 0.1 kHz
Bandwidth (-6dB)	2 kHz
Directivity	80 degrees
Sensitivity	-61 dBV/Pa (min)

The frequency response was then acquired for the ultrasonic transducers by pointing them directly at each other, separated by 3cm, and sweeping the input frequency of a signal on the transmitter from 1 kHz to 100 kHz. By doing this, it could be seen that the bandwidth of the transducers is verified at 2 kHz on either side of 40 kHz. With the sharp roll off thereafter, it would make detecting Doppler frequencies outside of this range difficult. See the frequency response of the transducers below:

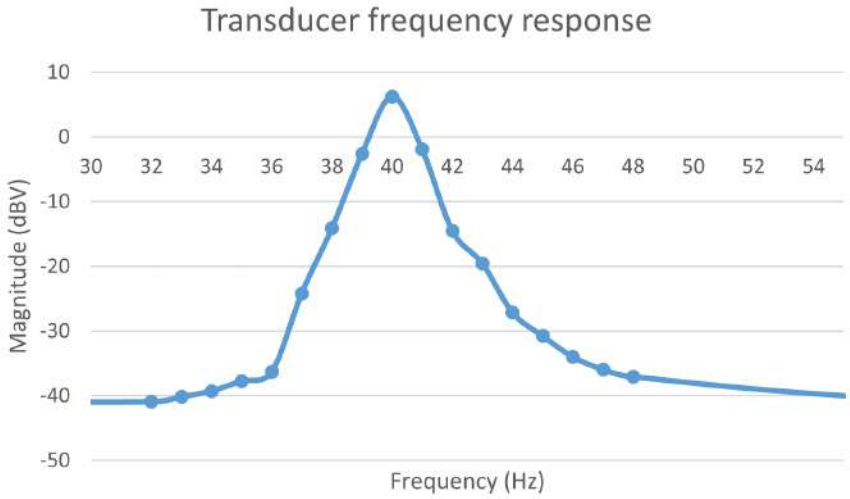

Figure 4.6: Frequency Response of ultrasonic barrel transducers obtained experimentally

Transmitter Design

The transmitter circuit filters the signal to be transmitted of unwanted frequencies and amplifies it before being transmitted by the ultrasonic transducer. The amplification is vital to emit a signal with enough energy to propagate through a required distance, and have an echo strong enough to be detectable by the receiver. The desired signal to be transmitted can be sampled and reconstructed by the XONAR U5, thus this circuitry concerns primarily filtering and amplification.

In order to achieve this filtering and amplification, an operational amplifier (opamp) needs to be chosen. An audio operational amplifier was used due to low noise characteristics. Furthermore, noting T.008 that the device must be powered from a 12V or 5V source, the power rails to be used were chosen as either +-12V or +-5V. The higher +-12V rails were decided on due to providing a larger possible amplification to the signal to be transmitted and received. Thus adds a parameter of the maximum output voltage (¿ 24V) when choosing the opamp. Thereafter, two other parameters are key in choosing the correct operational amplifier:

$$Slew\ Rate = 2\pi \times f \times V_{pp} \times 10^{-6}\ V/\mu s \tag{4.1}$$

$$Gain\ Bandwidth\ Product(GBWP) = 10 \times A_{cl} \times BHz \tag{4.2}$$

The slew rate, being the maximum rate of change voltage at the output of an opamp, was calculated noting that the max operating voltage is $+-12V$ therefore $V_{pp} = 24V$ and maximum frequency $f = 62157\ Hz$. This maximum frequency was obtained by noting the max frequency ranges for the system. Transmitting at 40 kHz and noting that the fastest recorded golf ball shot was 84 m/s [27] and choosing 95 m/s as the upper limit, one can calculate the Doppler frequency ranges when this speed is observed from a ball moving away and towards the RADAR:

$f_d = \frac{2v_r}{\lambda}\ with\ \lambda = \frac{c}{f} = \frac{3\times10^8}{40000}$
$\therefore f_d = \frac{(2)(95m/s)}{8.575\times10^{-3}m} = 22.1574\ kHz$

$\therefore f_L = f_C - f_d = 40\ kHz - 22.1574\ kHz = 17.843\ kHz$
$f_H = f_C + f_d = 40\ kHz + 22.1574\ kHz = 62.157\ kHz$

Thus now the slew rate can be calculated:

$$SlewRate = 2\pi \times 62157\ Hz \times 24 \times 10^{-6} = 9.373 V/\mu s$$

Regarding the GBWP as shown in equation (4.2), the closed loop gain can be calculated by noting the maximum peak to peak output voltage as 24 V and the maximum peak to peak input voltage as 3.3V. Thus $A_{CL}\frac{24}{3.3} = 7.27$. The bandwidth was calculated as the difference between the upper and lower maximum Doppler frequencies, $f_H - f_L$. This then gives a GBWP = 3.22 MHz.

$$GBWP = 10A_{CL}B = 10(\tfrac{24}{3.3})(44.314\ kHz) = 3.22 MHz$$

Given the GBWP and slew rate specifications, various opamps were considered:

- LM837
- LM6144BIN
- LT1359CN
- LT1214CN

All of the above opamps met the specifications, however the LT1214CN was finally chosen due to its low cost and availability as a quad op amp. See the LT1214CN specifications tabled below:

Table 4.6: Table of LT1214CN operational amplifier specifications

Parameter	**Specification**
Maximum Supply Voltage	36 V
Typical output current	30 mA
Typical slew rate	12 V/us
Typical GBWP	28 MHz
Low Input Noise Voltage	10nV/sqrt(Hz)
Total Harmonic Distortion	0.001%

Thereafter, the amplification and filtering stages could be designed for the transmitter circuit. It was determined that 1 amplification stage followed by 2 filtering stages would be sufficient. The amplification stage utilized an inverting adjustable gain amplifier in which the gain was set with a potentiometer R2 where the gain is thus $A_1 = -\frac{R2}{R1}$. Using a 10k potentiometer with a 1k resistor, a max gain of 20 dB can be obtained. Since the system designed is an LTI system, the gains of each stage are multiplied to obtain the overall gain or added in the dB scale. Thus, the amplification stage offers variable gain, whilst a later filtering stage includes built-in gain of 20 dB.

The filtering stages aimed to attenuate frequencies beyond the range of 38-42 kHz for the transmitter circuitry. Thus, a two stage active bandpass filter was deemed fit for this task. The first stage was designed to produce a gain of 0 dB, whilst the second stage was designed to produce a fixed gain of 20 dB.

The -3 dB point or half power point is defined as the cutoff frequency of the filter and are specified for an active bandpass filter as the low and high pass frequencies respectively:

$$f_{c1} = \frac{1}{2\pi R_1 C_1} = 30kHz \tag{4.3}$$

$$f_{c2} = \frac{1}{2\pi R_2 C_2} = 50kHz \tag{4.4}$$

The second filtering stage aims to improve this frequency response to be closer to 38-42 kHz whilst keeping 40 kHz in the centre of the frequency response. Values $f_{c3} = 34kHz$ and $f_{c4} = 48kHz$ were chosen to produce the desired response. Resistors of $120k\Omega$ and $12k\Omega$ were chosen to produce a fixed gain of 20 dB.
Circuit components were chosen according to what is readily available and common component values. Thus the Tx chain detailed in Figure 4.4 was designed as discussed. See the transmitter circuit below:

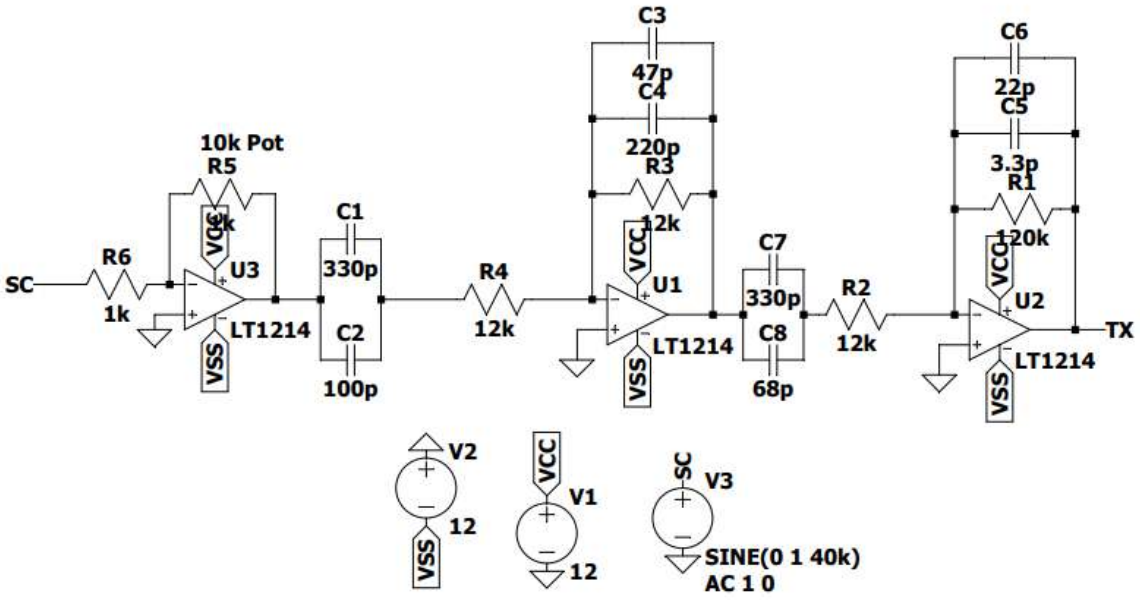

Figure 4.7: Transmitter circuit design

Transmitter Simulations

The first and second stage of the active bandpass filter was simulated in LTSpice as shown below:

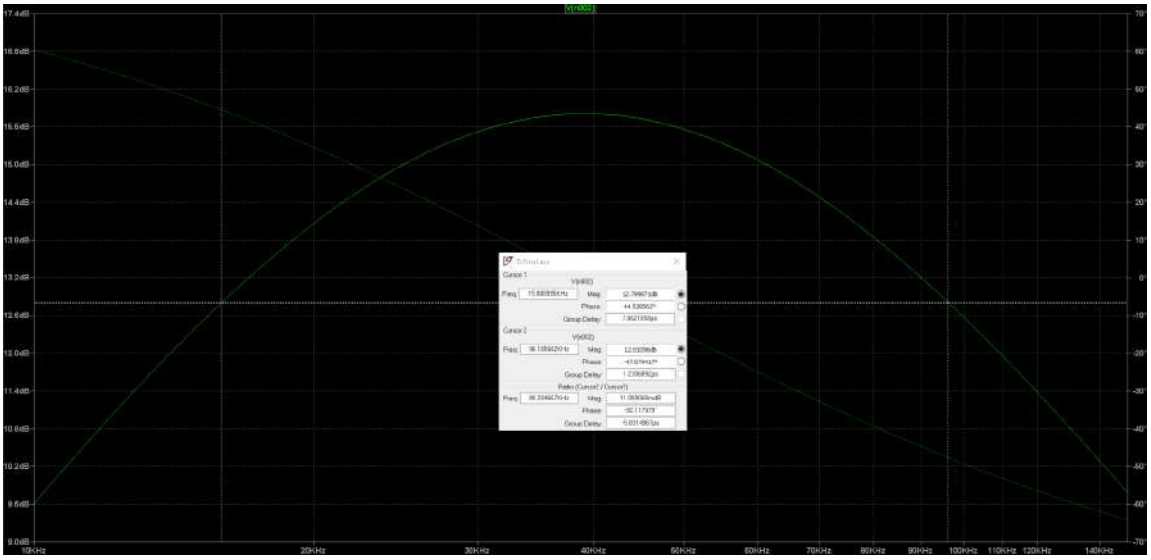

Figure 4.8: LTSpice simulated Tx 1st stage of BPF frequency response

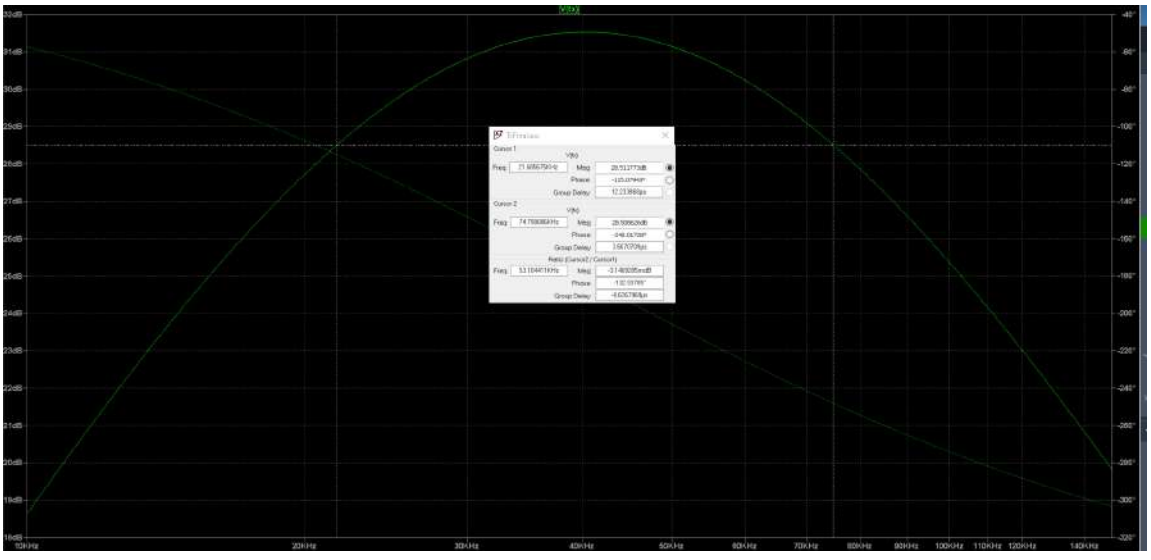

Figure 4.9: LTSpice simulated transmitter circuit overall frequency response

The above figures show that cutoff frequencies of 16 kHz and 96 kHz were obtained for the first stage, and 22 kHz and 75 kHz overall. This is in contrast to the designed cutoff frequencies of 30 kHz and 50 kHz, and 34 kHz and 48 kHz for the 2 stages respectively. This result however is adequate as it produces a response centred of 40 kHz and attenuates frequencies largely outside this range. The circuit could then be built and tested as shown below:

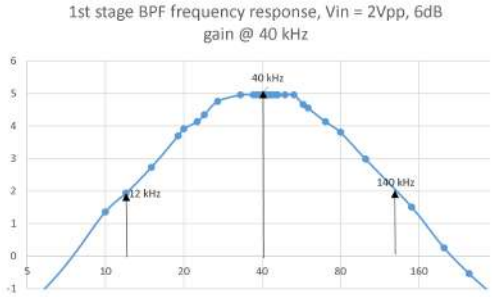

Figure 4.10: Tx 1st stage of BPF frequency response

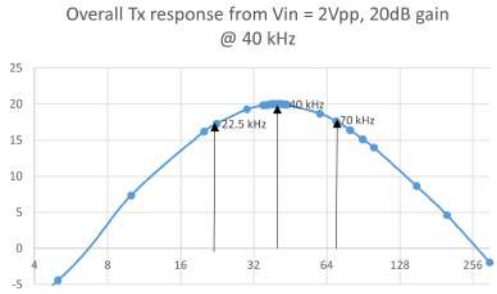

Figure 4.11: Transmitter circuit overall frequency response

As shown in the above Figures, the first stage cutoff frequencies are 12 kHz and 140 kHz, with the BPF response centred around 40 kHz. The overall frequency response is centred at 40 kHz with -3dB points of 22.5 kHz and 70 kHz respectively. The final circuit's performance matched expectations from the simulations and was determined to be adequate for the implementation.

Receiver Design

The receiver circuitry has a similar design to that of the transmitter circuitry except that it now receives echoes of the propagated signal, amplifies the attenuated echo, filters it of high and low frequency noise, modifies it to fit specifications and then sends it to the data acquisition card to be sampled. As seen in Figure 4.4, the receiver circuitry design has 4 main components:

- 20 dB variable amplification stage
- 2 stage active bandpass filter with 20 dB fixed amplification stage

- Clamping stage
- Clipping stage

The receiver circuit filter stages were then designed the same was as stated in the transmitter design section, with different cutoff frequencies now specified. The cutoff frequencies now need to accommodate the range of Doppler frequencies expected from 17.843 kHz to 62.157 kHz. Thus frequencies outside this range must be attenuated. Therefore, stage 1 cutoff frequencies were chosen as:

- $f_{c1} = 8kHz$
- $f_{c2} = 120kHz$

Stage 2 cutoff frequencies were chosen closer to the cutoff frequencies whilst attempting to keep the centre frequency at 40 kHz, and building in a fixed gain of 20 dB:

- $f_{c3} = 12kHz$
- $f_{c4} = 100kHz$

The clamping stage prevents negative voltages which may not be able to be sampled by microcontrollers used in future work, and the clipping stage protects the microcontroller/DAQ from high voltage signals over 3.3V. The clamping stage was designed to clamp the input signal to oscillate around 1.65V or 3.3V/2 with a voltage divider. A steady 3.3V supply is thus needed for this, and was designed using an inverting op amp with a variable gain using a potentiometer and a 12k resistor. Thus the clamping point can be adjusted. It is important to note, that the output of the op amp is decoupled to ground with a 100 microfarad capacitor to prevent voltage spikes, and a 12k resistor is included in series between the filtering stage and clamping stage otherwise the clamping circuit opamp would need to able to sink enough current to overcome what the filtering stage opamp can source - causing the outputs to fight each other. Including the 12k resistor prevents the clamping circuit op amp from going into current limiting as well.

The clipping stage makes use of two 1N5819 schottkey diodes, one biased with the 3.3V input and the other to ground. This clips the output to around 3.3V and ground (not perfectly due to the voltage drop over the schottkey diodes, but the XONAR U5 can handle negative voltages).
The full receiver circuit design can be seen below:

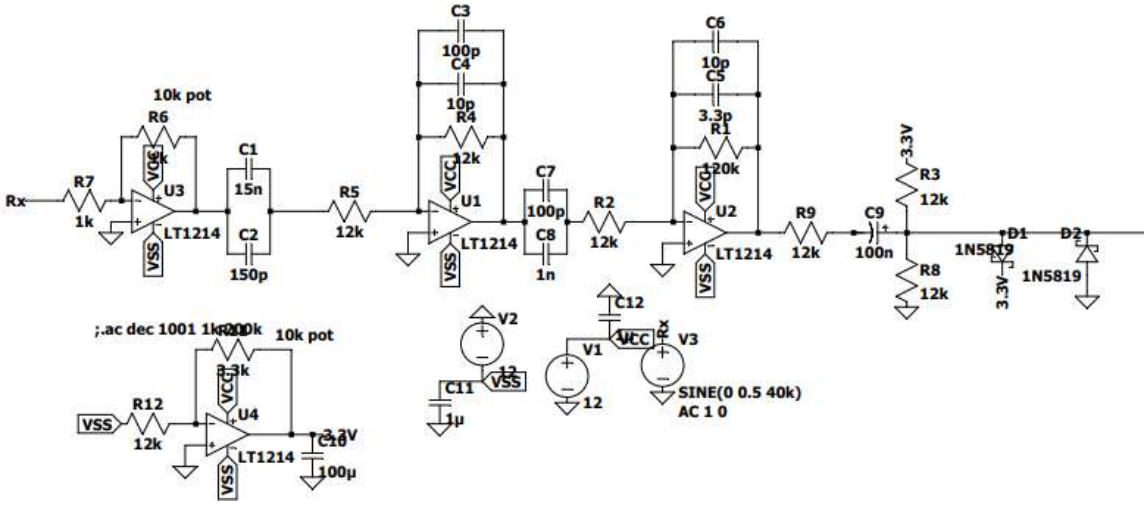

Figure 4.12: Receiver circuit design

4.2.5 Receiver Simulations and results

The first and second stage of the active bandpass filter was simulated in LTSpice as shown below:

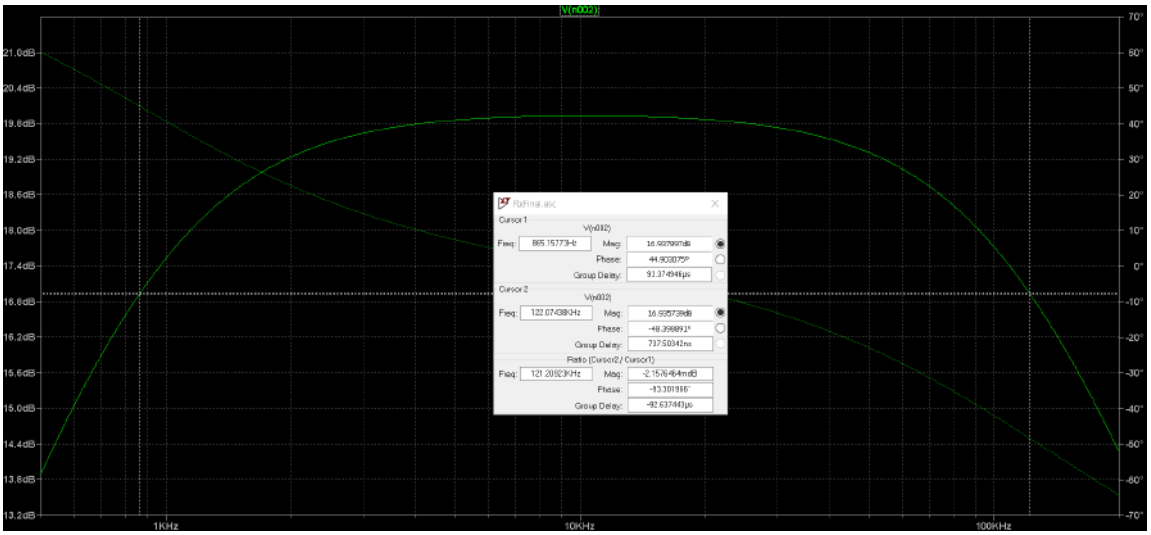

Figure 4.13: LTSpice simulated Rx 1st stage of BPF frequency response

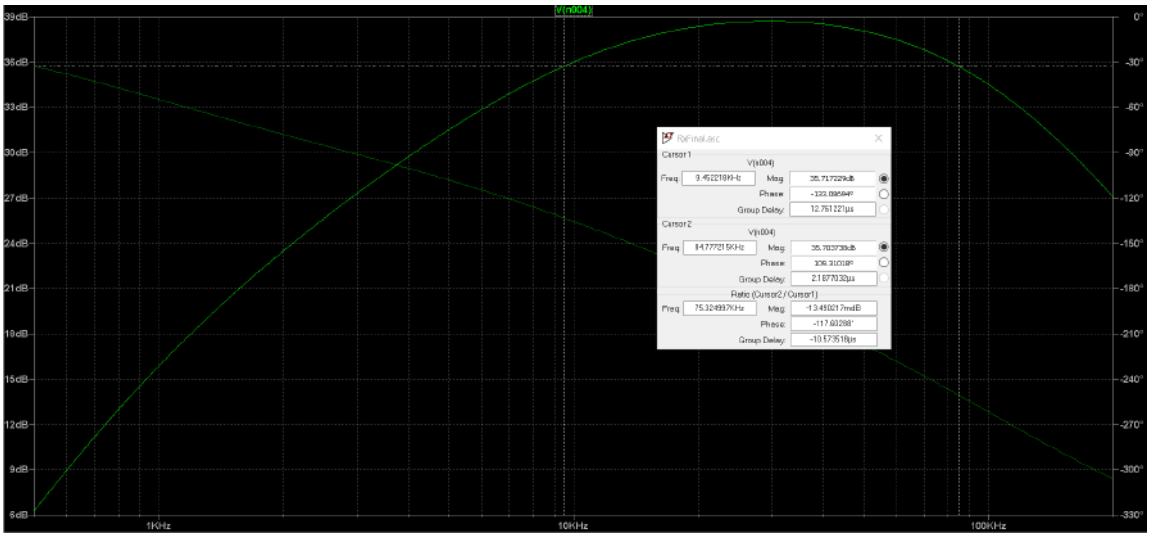

Figure 4.14: LTSpice simulated receiver circuit overall frequency response

The cutoff frequencies from the simulations are 865 Hz and 122 kHz for the 1st stage, and 9.5 kHz and 85 kHz for the 2nd stage. The circuit was designed for 8 kHz and 120 kHz for the 1st stage and 12 kHz and 100 kHz for the 2nd stage. The simulations provide adequate performance from the calculations - frequencies outside the upper and lower Doppler frequencies for the system are attenuated significantly whilst 40 kHz is maintained at a higher gain close to the centre of the peak of the response. The first stage of the BPF and the overall circuit frequency response was measured as shown below:

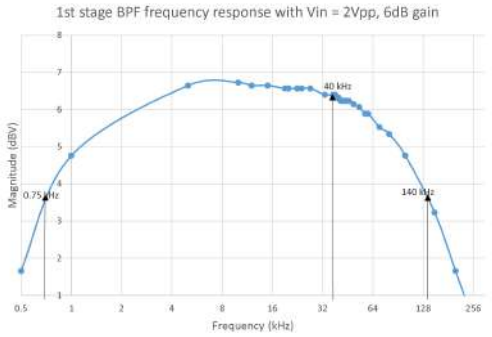

Figure 4.15: Rx 1st stage of BPF frequency response

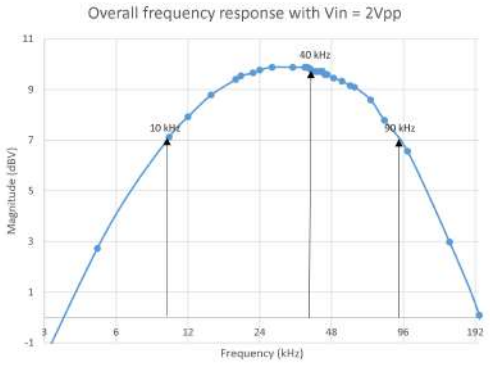

Figure 4.16: Receiver circuit overall frequency response

The above figures show that cutoff frequencies of 0.75 kHz and 140 kHz for the 1st stage and 10 kHz and 90 kHz for the overall response. Thus the built circuit performed very similarly to the simulated circuit and thus met the desired design criteria.

The receiver circuit also implemented clipping and clamping circuitry. As shown in the 1sst figure below, an input 40 kHz signal of 0.5 Vp can be amplified up to within the range of 0-3.3V (adjustable gain of 20 dB), and is clamped at around 1.6V. It is shown to oscillate around 1.65V due to the voltage drop across the Schottkey diodes. This can be adjusted by tuning the potentiometer in the 3.3V-producing inverting opamp circuit. The 2nd figure then shows the clamping action of the clamping circuit working as a result of the Schottkey diodes.

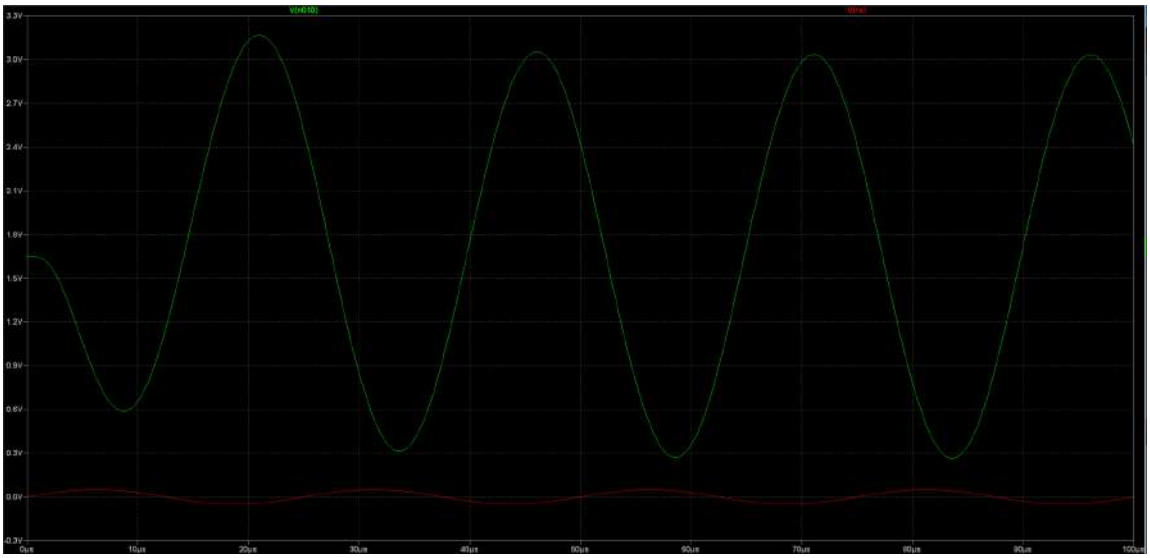

Figure 4.17: Receiver circuit output in response to a 0.5 Vp 40 kHz signal input

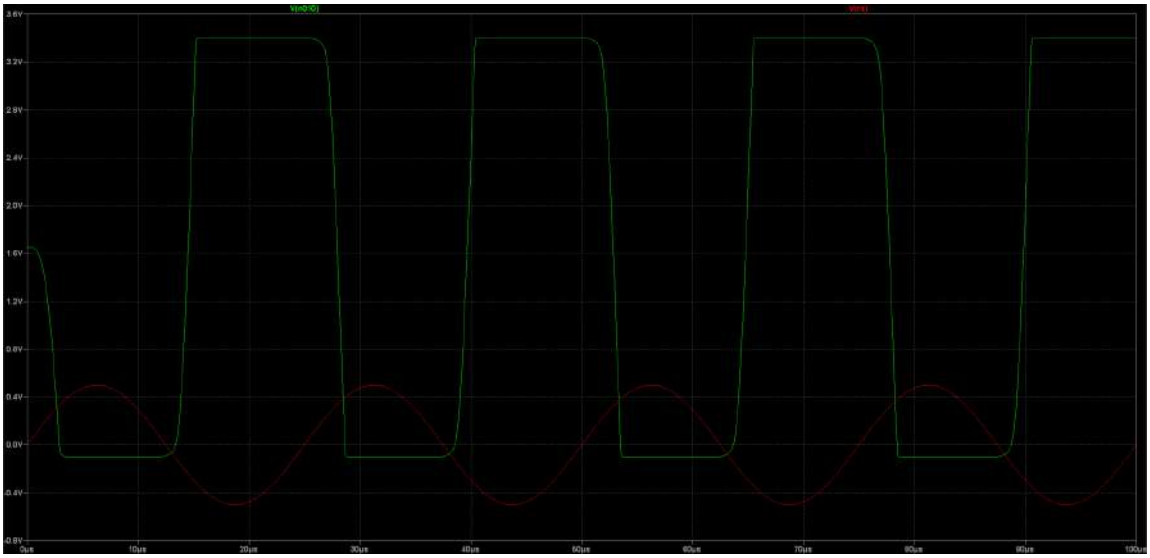

Figure 4.18: Receiver circuit clipping action on too large an input signal

Power Supply Design

As per T.008, the ultrasonic device needs to be powered from a 12V or 5V battery supply. The user provided a 12V/5V power bank and is detailed below:

Table 4.7: Table of Technical Specifications

Parameter	Specification
USB Output	5V 2.1/1A
Car boor port	12V
Input	CC/CV 15V/1A
Peak Current	400A(<3S)
Size	165x75x30mm (WxHxD)
Capacity	12000mAh

Figure 4.19: Mini car charger power bank

As observed in the transmitter and receiver designs, the LT1214CN Quad operational amplifier was chosen to run off of +-12V dual supply rails. Thus, the power supply circuitry needs to regulate a possibly fluctuating output 12V, and produce +-12V. This section describes how this is accomplished with a 12V power bank, boost converter and active rail splitter circuit.

Various options were explored to produce a dual rail supply such as a charge pump, switched capacitor converters and active rail splitter circuits. Due to time and budget constraints and the ease of the solution, a common active rail splitter was selected. A typical method of obtaining a dual supply is to split double the voltage using rail splitter circuitry. Since the output of the battery is only 12V, it needed to be boosted to 24V then split into +-12V. The boost converter would output 12V at its setpoint despite fluctuations at the input, however switch mode regulators such as a boost converter tend to have high switching frequencies which introduce large amounts of noise into the circuit. Thus ideally, one should regulate one's dual rails on the output. However the only linear regulators on hand were the LM7812 and LM7912 which require a minimum input voltage of 14.5V due to the high dropout voltage. (CITATION NEEDED FOR LM7812 and LM7912) Various circuits were

thus considered with the boost converter to combat this issue:

- Using Low Dropout (LDO) linear regulators on the output - low dropout voltage.
- Using a bigger boost converter that could boost 12V to 36V then using the LM7812 and LM7912 to produce regulated +-12V.
- Using an LM317 adjustable regulator instead of the LM7812, however this requires extra components to produce the setpoint.
- Use a master's student's board that produces +-9V from a 5V input.
- Use only the boost converter, and measure the output noise to see whether or not it will affect the supplied circuitry.

The easiest and most efficient choice given time constraints was to first characterize the boost converter's output to determine if regulating its output was necessary. The FFT shown below captured on an oscilloscope shows how low power the noise is at the frequency range of interest. Thus no linear regulators were used at the output of the boost converter, however it would be ideal to include them in any case.

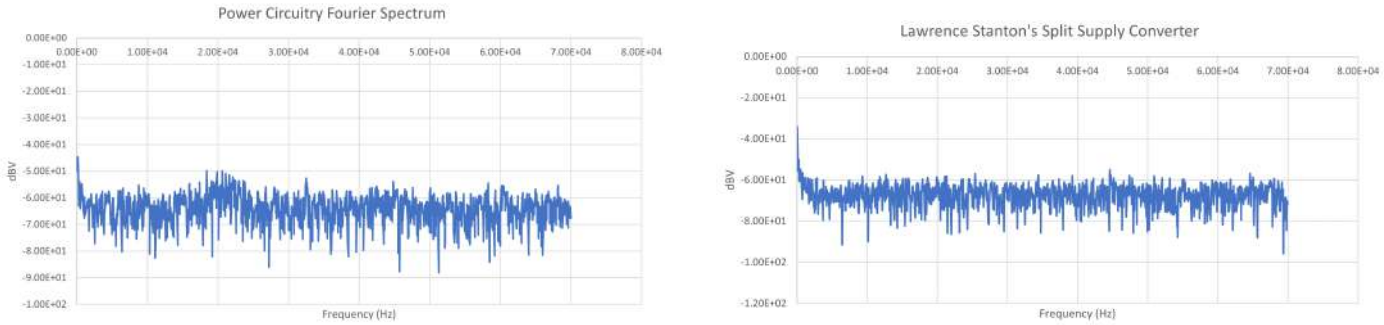

(a) Custom Split Rail Supply Circuitry Output

(b) Lawrence Stanton's PCB output

Figure 4.20: Comparison of custom dual rail supply circuitry versus Lawrence Stanton's PCB

Thus an MT3608 Boost Converter was chosen due to its low cost and availability on hand in the lab, and relatively similar performance to that of the PCB provided from Lawrence Stanton. Thereafter, an active rail splitter circuit was built using a LT1214CN operational amplifier since it was used in the transmitter and receiver circuitry and was thus on-hand, and allows for an output voltage swing of 0-24V. The output of this circuit successfully produced +-12V with reference to a virtual ground. This virtual ground was then used as the ground point throughout the transmitter and receiver circuits. See the figure below:

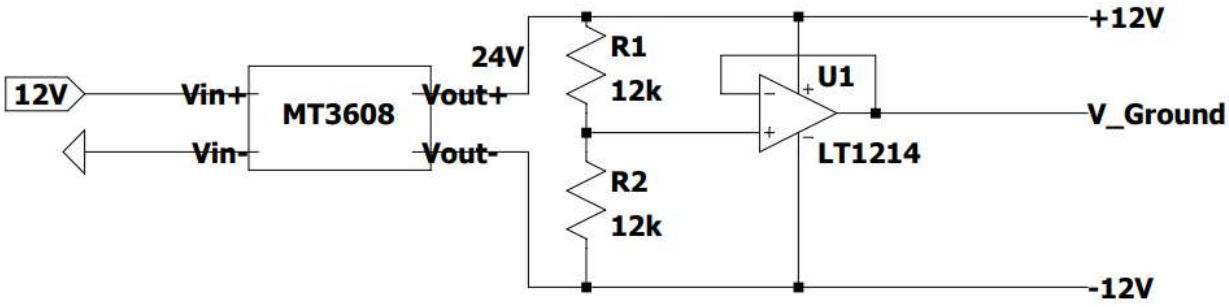

Figure 4.21: Power circuitry design to obtain +-12V from 12V power bank

The power rails on both transmitter and receiver circuits were decoupled with 100 nF ceramic capacitors with respect to each other and to ground to prevent large voltage spikes and fluctuations in the output.

4.2.6 Enclosure Design

As per T.003, the device needs a robust enclosure to protect it from the elements and be used outdoors. The enclosure would need to house the power supply, transmitter, receiver and power supply circuitry, sensors, audio jacks, a switch and a status LED for user friendliness. Ideally, the power supply should be able to be accessed and charged or even removed, with ease.

The enclosure was envisioned to meet the above requirements, whilst also properly mounting the ultrasonic sensors, having enough space for different uses in the future,

separate the power bank, jumpers connected to the power bank and strip-board circuits from each other and allow for cable management. Thus three compartments were decided on: A front compartment for the transmitter, receiver and power circuitry strip-boards, a middle compartment for the jumper cables to sit side by side connected to wires from the power circuitry, and lastly a back compartment that houses the power bank. A lid would be designed to cover the enclosure but leave a slot open for the power bank to be recharged easily.

The enclosure was designed following the transmitter and receiver being designed and soldered to strip-board. This provided the dimensions necessary for the enclosure. The height of the enclosure was determined by the height of the power bank - 75 mm + space for cables therefore 105 mm. The length of the enclosure was again determined by the length of the power bank (165 mm) and allowing for space holes for self tapping screws for the lid to attach. Thus the length was set to 190 mm. The breadth of the enclosure was a summation of the breadth of the widest strip-board circuit, the breadth of the power bank, the breadth of the jumper cables sitting side by side, breadth of the slots to separate the power bank, jumpers and circuits as well as the breadth of the exterior enclosure walls. This all resulted in a breadth of 148 mm. Thus the final dimensions of the enclosure came to 190 x 148 x 105 mm. The figure below shows technical drawings generated for the model, designed in Fusion 360. A 3D shaded model of the enclosure can be found in the appendix.

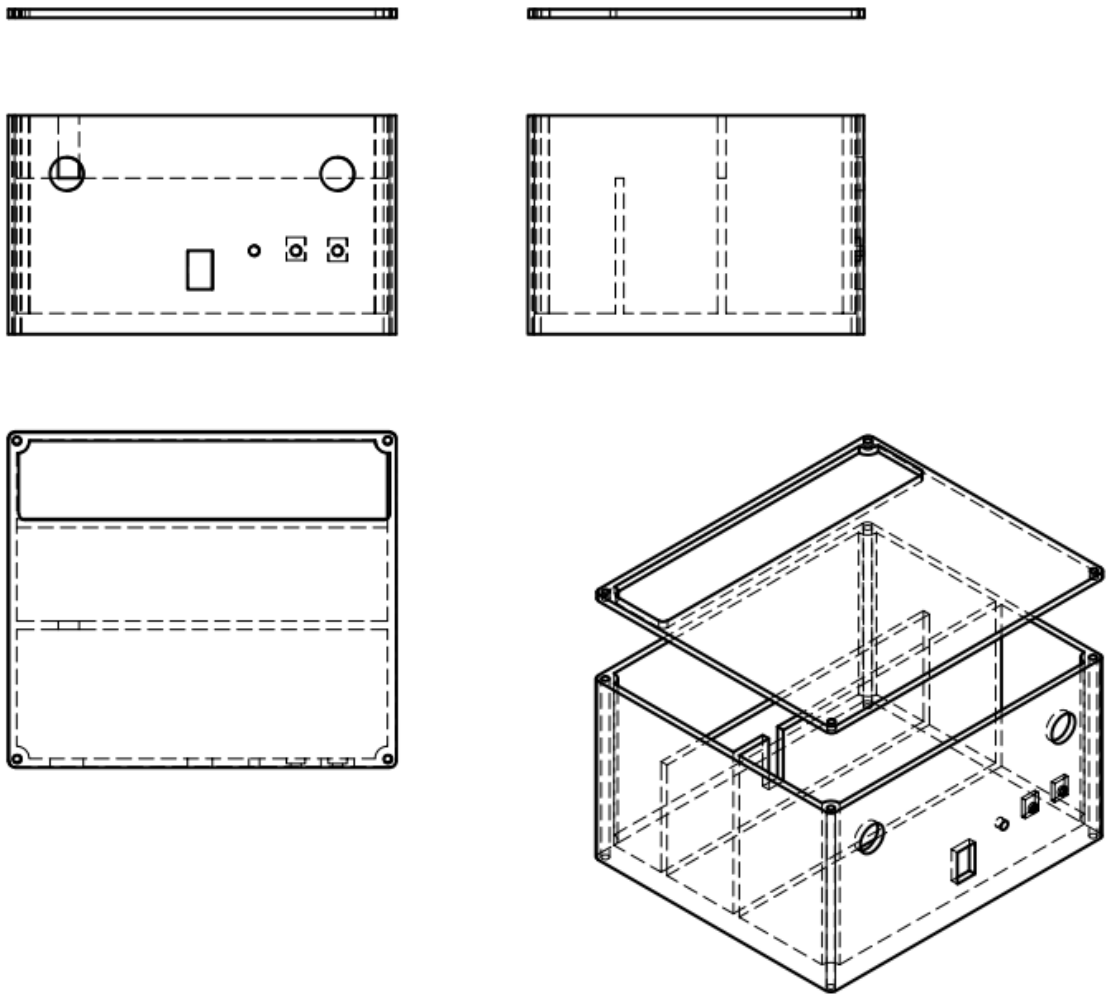

Figure 4.22: Fusion 360 generated technical drawing of the designed enclosure

The enclosure material needed to meet T.003 of being robust for outdoor use. Obvious materials for this use case include wood and plastic materials. However, taking into account the availability of 3D printers on campus and the ease thereof of getting most desirable shapes with a relatively fast turnaround time, a 3D printing approach was chosen. The design was printed using black PLA filament, with a 0.4 mm nozzle being used on an Ender 3 at 100% infill. Following printing, rough edges were filed down and the components were mounted successfully and fit well - proving the speed

and efficiency that 3D printing provides for prototyping. The lid was mounted and screwed down onto the enclosure with 5mm diameter self-tapping screws.

The figures below show the fully built hardware system, including the transmitter, receiver and power supply circuitry soldered to strip-board and mounted in the enclosure.

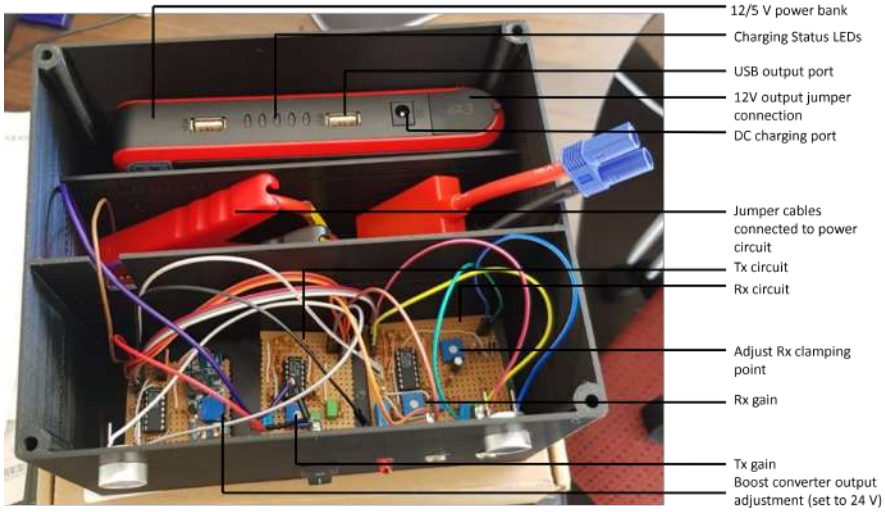

Figure 4.23: Interior view of the finished hardware system

Figure 4.24: Front view of the finished hardware system

Figure 4.25: Top view of the finished hardware system

4.3 Signal Processing Design

The signal processing performed in the system is tailored towards a CW Doppler ultrasonic RADAR as discussed, but with the limited scope of not needing to operate live continuously. Thus, there are a few key stages are used to transmit, receive and process the signal. These key stages are shown in the signal processing flow diagram below:

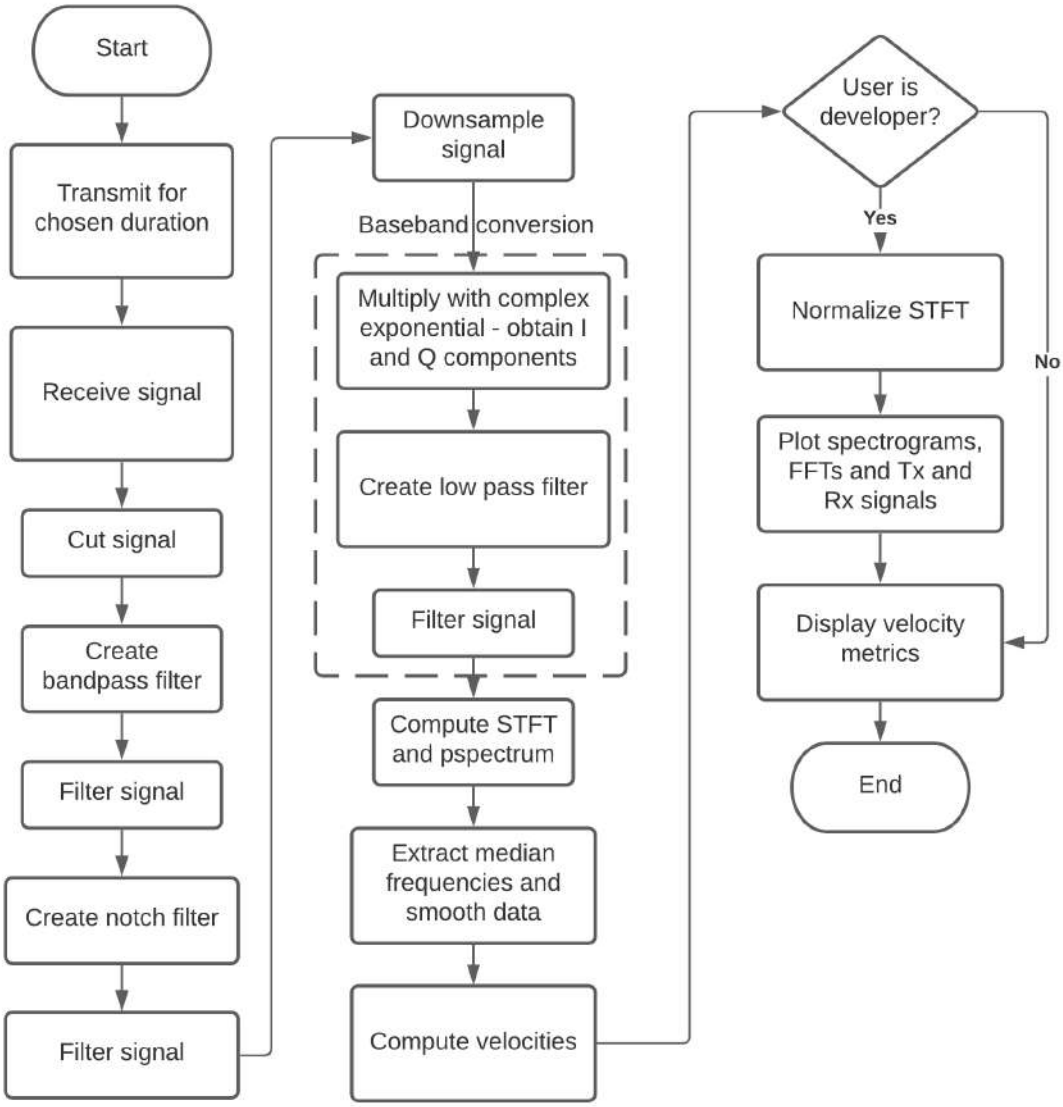

Figure 4.26: Signal processing flow chart

A visualization of the FFT of the signal after each stage of processing is shown below and will be used in the discussion of the signal processing design:

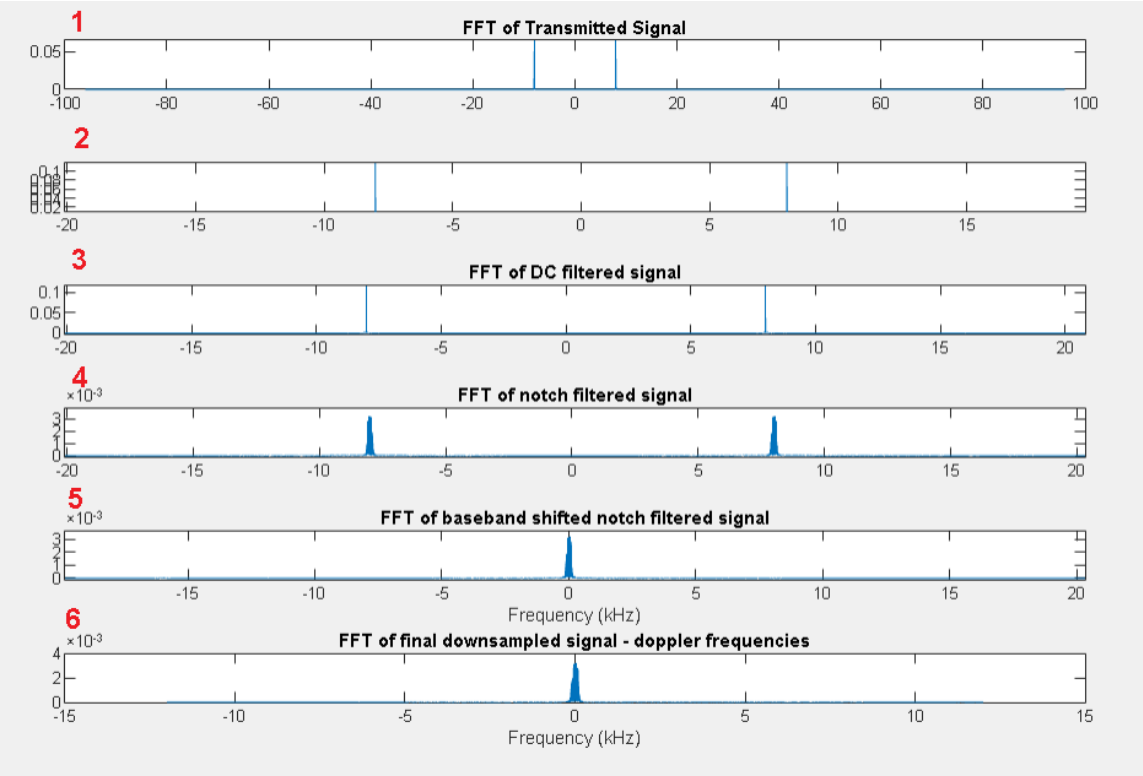

Figure 4.27: Key steps in signal processing

Firstly, the desired signal is transmitted and received over a certain amount of time. The transmitted signal is seen in 4.27 at 1. The received signal has its first 0.2 seconds cut as this accommodates startup time of the sound card. Thereafter, any DC offset and noise around DC is filtered out using a 6th order Butterworth band-pass filter around 40 kHz with cutoff frequencies around the upper and lower Doppler frequencies, see 3 in 4.27. Furthermore, any remaining DC offset is removed by removing the mean of the signal from itself. The BPF filter's frequency response is shown below:

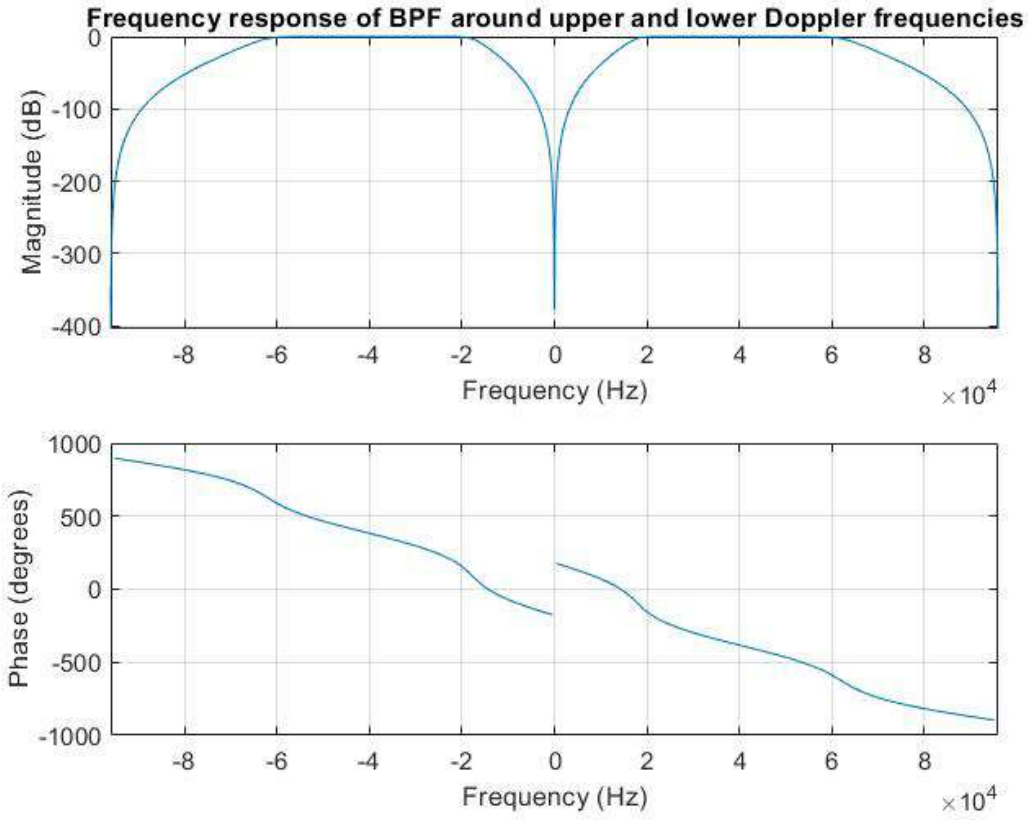

Figure 4.28: Bandpass filter used to remove DC components received in the signal

Thereafter, a notch filter is used to filter out received high power "clutter", i.e. non-moving targets, from as close to 40 kHz as possible. By doing so, it is far easier to observe Doppler frequencies around 40 kHz. See the output of removing clutter at 4 in 4.27 and the frequency response of this notch filter below:

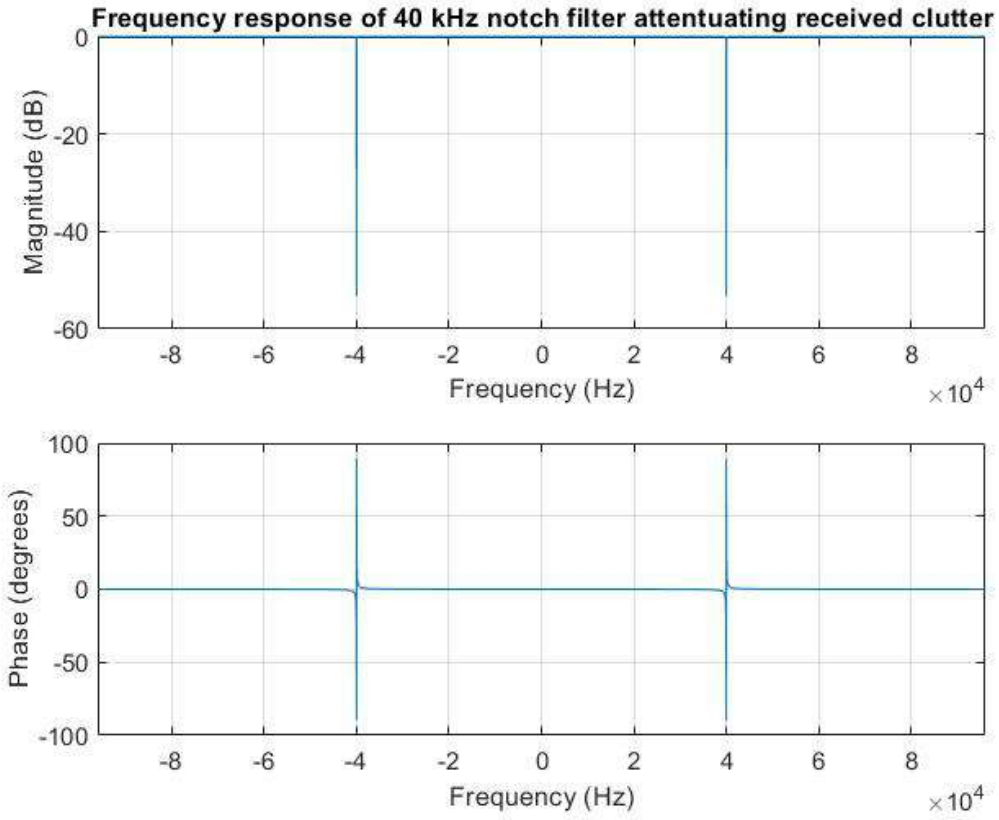

Figure 4.29: Notch filter used to remove 40 kHz clutter in the received signal

Hereafter the signal is base band shifted by multiplying the signal by orthogonal sinusoids at the centre frequency thereby modulating the signals to base-band and producing real and imaginary (I and Q) components. The components are used to form a complex signal again and the signal is low pass filtered to remove components modulated to higher frequencies ($2\omega_0$). See number 5 in the diagram in 4.27. Now that the signal is at 0 Hz and filtered of all clutter, Doppler frequencies or frequencies that have shifted slightly above or below 40 kHz can be easily observed in the spectrum.

Now that the signal is at base-band, the present frequencies are much lower than that of the original signal, thus the Nyquist sampling rate required is much lower. Thus

the signal is down-sampled by a factor of 8 to reduce the size of the data set but still keeping useful information therein (Number 6 in diagram). The signal processing discussed thus far is performed by a processDoppler function shown here A.1 in the Appendix. Because the signal will exhibit brief frequency changes over time during the lifetime of a ball passing through the air towards or away from the RADAR, it becomes necessary to plot frequency as a function of time to observe when certain Doppler shifts become evident in the spectrum. Thus a spectrogram is used to show the frequency spectrum of the data as a function of time. An STFT is used which repeatedly calculates the DFT of a signal over a window of the data, and shifts it, producing many DFT results for a number of time slices.

A Compute_STFT function was designed to receive the signal of interest, the sampling rate, size of a window and an overlap factor. It then calculates the number of frames to be taken from the data set given the size of the data set, window size and overlap factor. A 2D array is prepared to store DFT values associated with time and frequency. Then looping through the number of frames, a hamming window is applied to a portion of the data equal to the given window size, and then an FFT is taken of the windowed data, zero padded, the first half taken and multiplied by 2 to provide a single sided spectrum of the data. The spectrogram and transmitted signal parameters can be customized in the developer GUI as detailed in the next section.

Hereafter, a threshold is applied to remove any noise below a certain calibrated dB level, and the maximum velocity is obtained by stepping through the time frames and finding the highest amplitude STFT value and storing its associated frequency. The maximum frequency found is recorded and converted to velocity with equation 2.4. The mean velocity is calculated by taking a moving mean over the data set of a medium size window, and taking the max thereof - this prevents speeds recorded over a short time in a long time recording to be masked by a typical mean calculation. A spectrogram is then used to plot a normalized version of the STFT matrix as shown in 4.32.

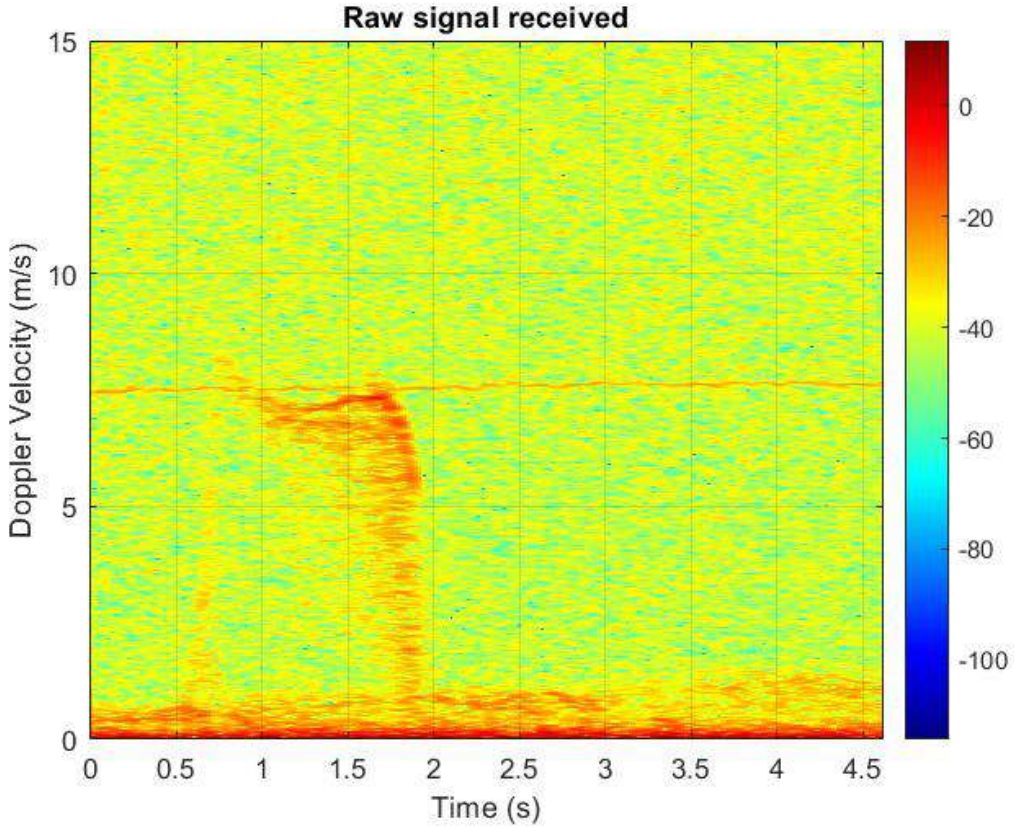

Figure 4.30: Raw STFT output before thresholding and smoothing, plotted as a spectrogram

This method of obtaining estimations of instantaneous, maximum and average velocity is compared with that of using MATLAB's pspectrum function which accepts the sampling frequency, frequency axis, input time domain data, frequency resolution and threshold in dB, and returns power spectrum, frequency and time arrays. Simply calling pspectrum with 'spectrogram' as a parameter plots a spectrogram. By using the 'medfreq' method on the returned power spectrum, one can obtain an array of frequencies which correspond to the median frequency for each frame in the power spectrum matrix. This is useful as the median represents the midpoint in the power distribution and is thus a useful tool in extracting the frequency estimates and thus velocity estimates from a noisy spectrum. The Doppler frequencies have

more power than the surrounding noise and can thus be extracted with 'medfreq'. See the pspectrum output shown below compared with the custom STFT plotted as a spectrogram:

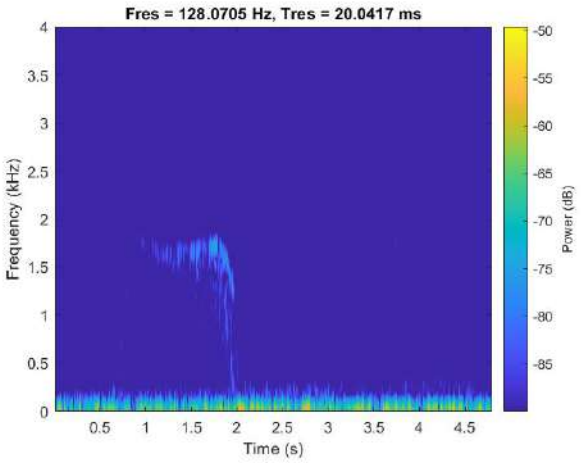

Figure 4.31: MATLAB pspectrum output

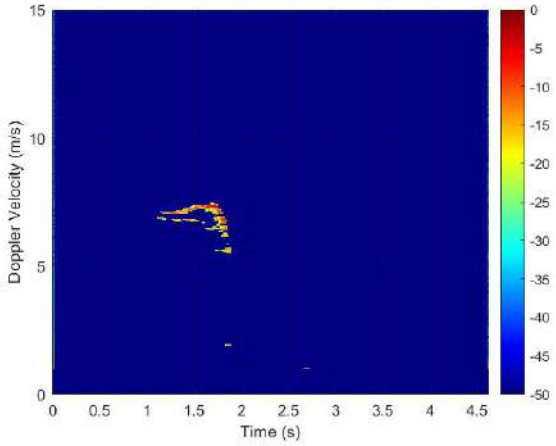

Figure 4.32: Normalized STFT output plotted as a spectrogram of velocity versus time

4.4 GUI Design and data logging

A GUI is required as per T.006 in 1.1. Two MATLAB Applications were designed using MATLAB's App Designer tool - a Developer_Demonstrator application and a Demonstrator_App. This was to make testing and data collection easier, with the Developer_Demonstrator application allowing the user to change the spectrogram parameters, and sampling parameters easily without having to restart the application or alter code. The Demonstrator_App removed technical parameters and simplified the interface such that any user could use it with ease.

The Developer_Demonstrator App allowed one to specify the transmitting frequency, the time to transmit, the sampling frequency, spectrogram number of samples per frame and overlap percentage. It also then displayed the custom algorithm outputted

max, average and instantaneous velocity estimates, along with the medfreq method's max, average and instantaneous velocity estimates. The app has two other tabs for the developer to view the fourier spectrum of the signal throughout the signal processing and a tab to view the transmitted and received time domain signal. See the developer application below:

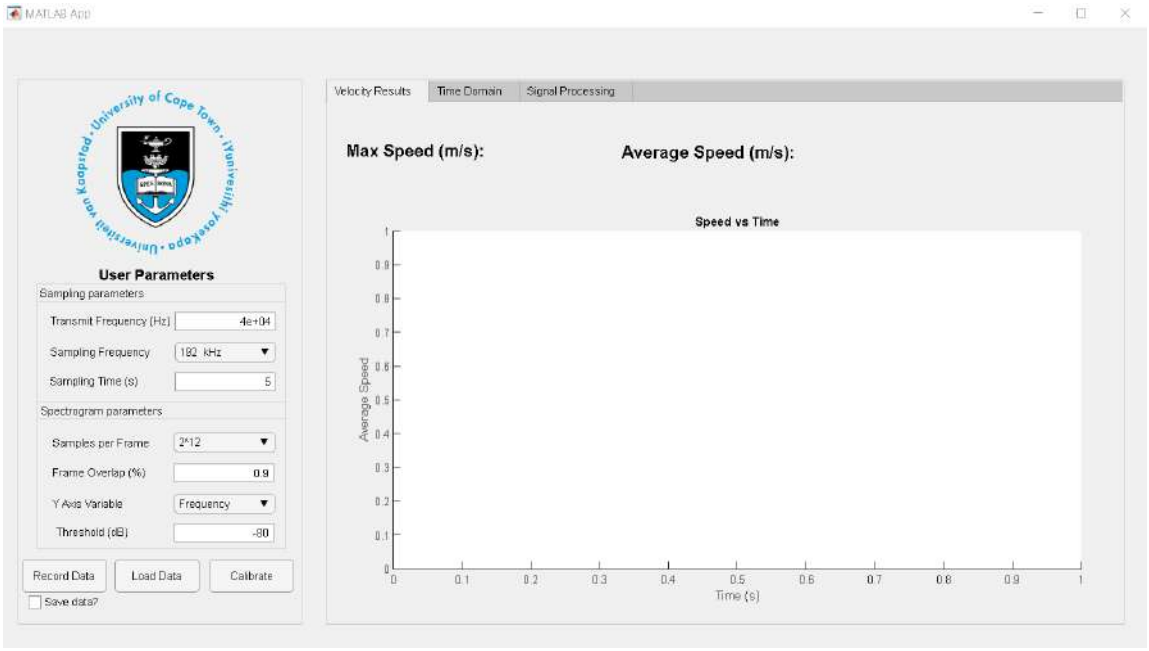

Figure 4.33: Developer_Demonstrator application interface

The Demonstrator GUI to meet the user's needs was a simplified version of the above GUI, removing technical parameters and allowing the user to simply adjust the time to record. The velocity estimates and instantaneous velocity is outputted. See the GUI below:

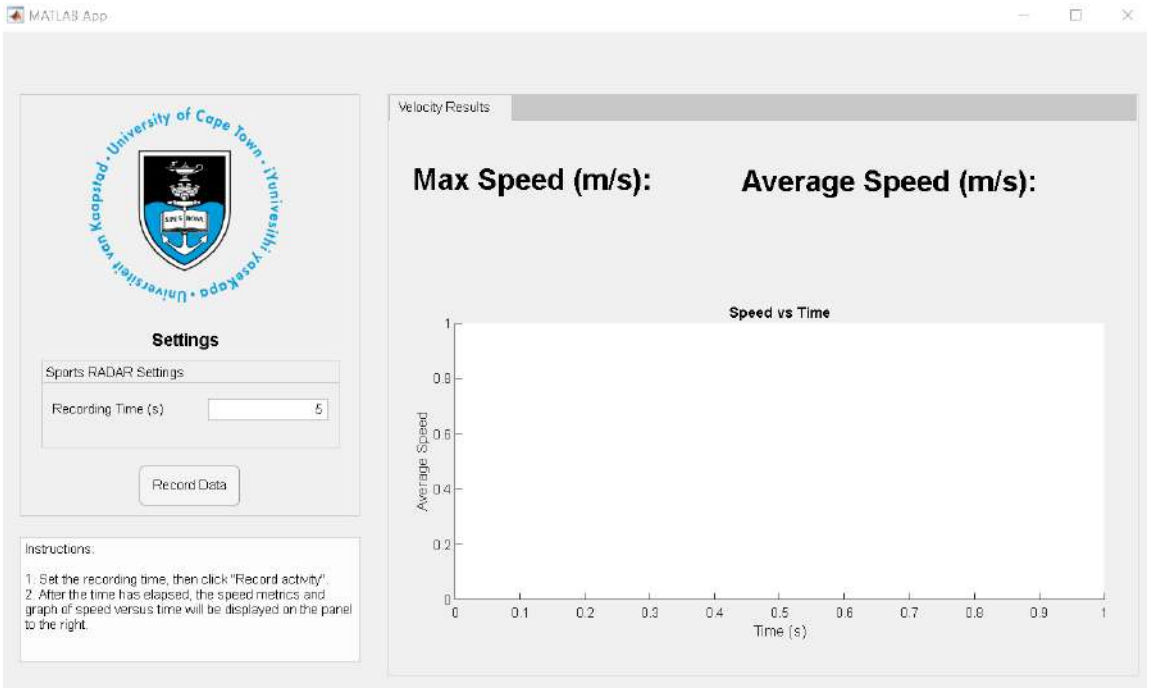

Figure 4.34: RADAR Demonstrator user interface

During experiments a lot of data will be stored for many different experiments. Thus a script was written called dataextraction.mat to process the velocity estimates from all the data sets found in a chosen directory and store them into a .csv file for easier processing thereafter.

Chapter 5

Results

5.1 Experiments and Results

5.1.1 Experimental Setup

As discussed in the methodology, the ideal transmit frequency, the ideal noise threshold for various environments, minimum ball size (RCS) detectable, the best velocity estimation algorithm and maximum range was to be determined experimentally. After the design of the hardware, signal processing and GUI was complete as detailed in the Design section, the experiments could now be completed. For all results obtained, uncertainty and error was propagated through the calculations to provide an uncertainty interval for each measurement. The results and their intervals were compared to see if they overlapped and "agreed within a reasonable degree of uncertainty". See below the uncertainty formulae used:

- Uncertainty when reading off a digital instrument:

$$u(D) = \frac{x_{upper} - x_{lower}}{2\sqrt{3}} \tag{5.1}$$

- Uncertainty when reading off an analogue instrument:

$$u(A) = \frac{x_{upper} - x_{lower}}{2\sqrt{6}} \tag{5.2}$$

- Equation to combine uncertainties (with $R = c.A^a.B^b$):

$$u(R) = R.\sqrt{[a\frac{u(A)}{A}]^2 + [b\frac{u(B)}{B}]^2} \tag{5.3}$$

In order to collect data for the experiments described in the methodology, 3 experiments were done namely An indoor test and two outdoor tests. The indoor test consisted of dropping balls of different sizes (a rugby ball, tennis ball and squash ball) over heights of 1m, 2m and 2.5m whilst recording with a camera and with the audio and ultrasonic systems. The figure below shows the experimental setup. Note that the figure shows the camera's perspective.

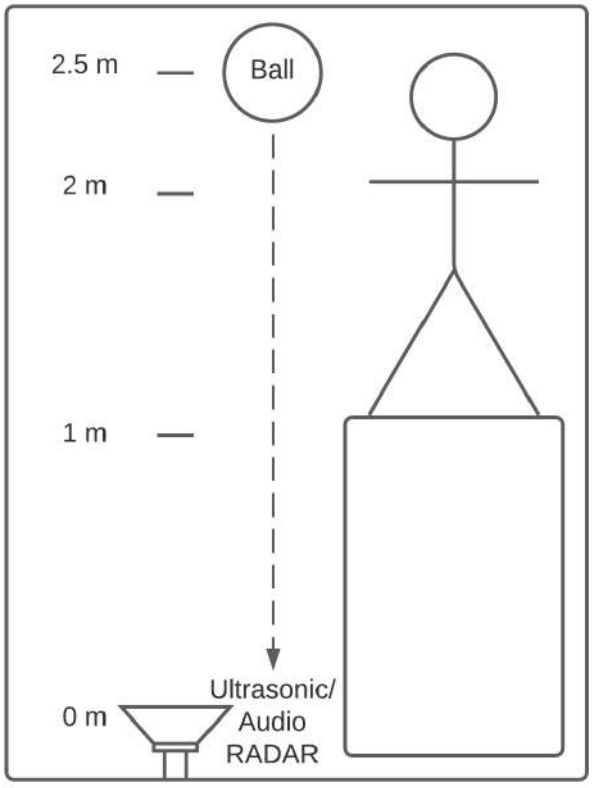

Figure 5.1: Indoor test setup

Two outdoor tests were carried out as well. The first outdoor test, tabled on the next page, was considered unreliable data and thus discarded as the video recordings were taken in the direction of the movement of the ball - this made extracting the start and stop times of the ball's travel difficult and unreliable. Thus velocity measurements produced cannot be said to be accurate. A second set of outdoor tests were then carried out with the video recording from a profile view, with different balls of different sizes thrown or kicked over distances of 6m and 10m. The video, audio and ultrasonic systems were used to record each experiment simultaneously. See the figure below describing the outdoor experiment setup:

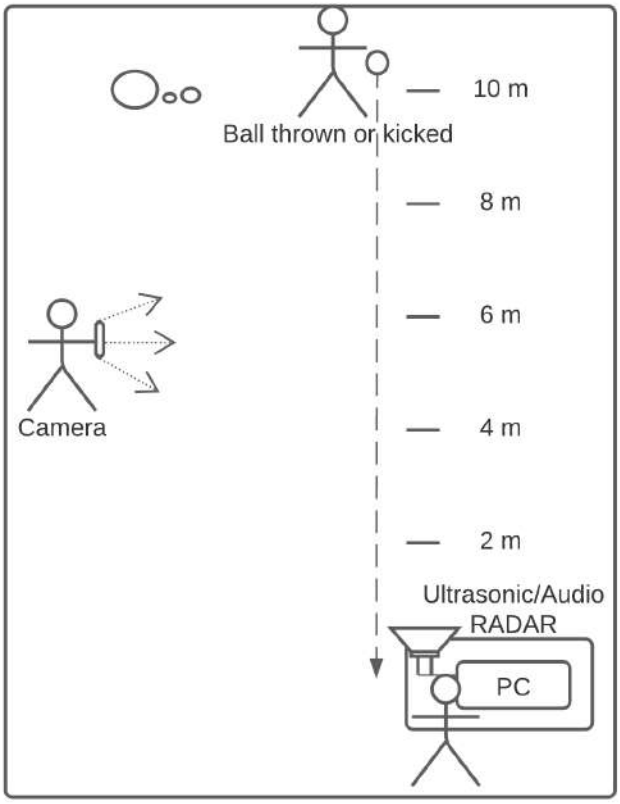

Figure 5.2: Outdoor test setup

5.1.2 Experiment Walkthrough

In this example, a basket ball is thrown outdoors over 10 metres and recorded with the ultrasonic system at 40 kHz like in 5.2. Firstly, the system is setup as follows:

1. The XONAR U5 soundcard is powered from the PC via USB.
2. An AUX cable connects the Tx port of the ultrasonic system (see 4.24 to the soundcard's headphone jack. Another AUX cable connects the Rx port of the ultrasonic system to the mic jack of the soundcard.
3. The ultrasonic system is aimed in the direction of the incoming ball, at a reasonable expected height of the ball, and turned on.
4. The MATLAB Demonstrator_App is then opened. For testing, the developer version was used. The parameters are set - for this example, a 40 kHz signal is transmitted and sampled at 192 kHz for 5 seconds.
5. RECORD is then clicked on the application and the ball is then thrown during the transmission period.

The following figure shows the GUI setup and output velocity:

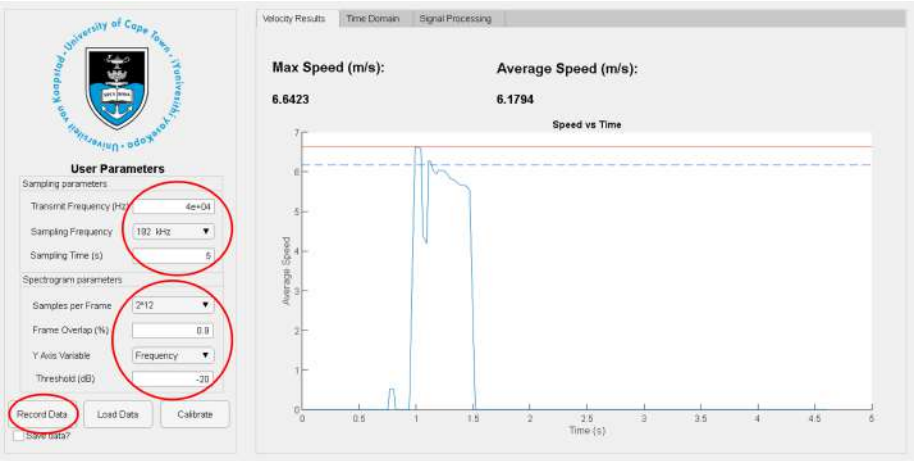

Figure 5.3: GUI setup for experiments

The custom algorithm uses the chosen spectrogram parameters, shown in the red circles above, with the threshold being set by the calibrate function and fine tuned through experiments thereafter. The rest of the experiment walk-through includes a comparison between the custom STFT approach and the "medfreq" approach as detailed in the methodology 3.4.3. After the initial signal processing stages are completed on the received signal (shown in 4.27), the custom STFT function and MATLAB pspectrum function can be used to output spectrograms of the raw received signal:

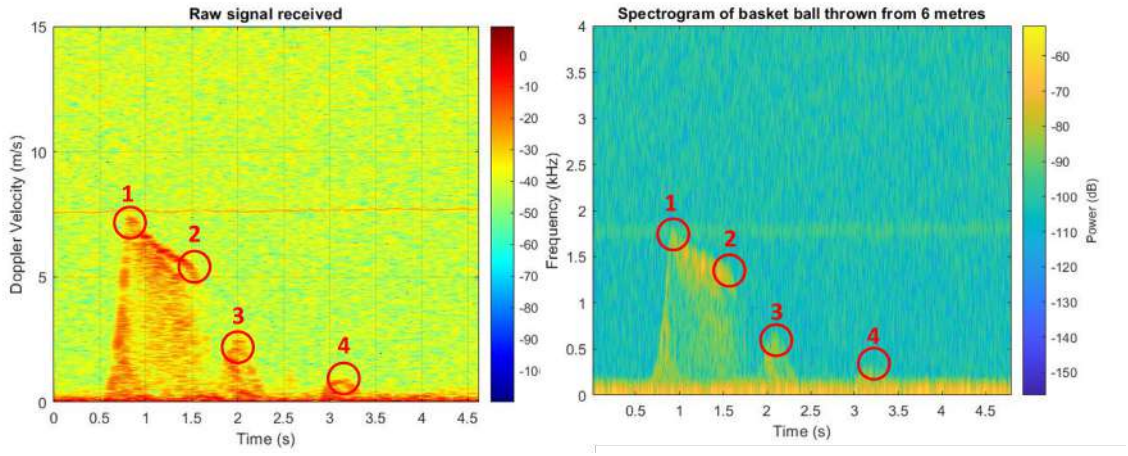

Figure 5.4: Received signal before thresholding, with custom STFT versus MATLAB "pspectrum" output

In the spectrogram, the darker red patches in the left diagram show areas of greater STFT magnitude in dB and more yellow patches in the right diagram show areas of greater power in dB. The scale alongside gives a measure of the power in dB and its associated colour. The background noise power can also be read off - in the left diagram it is seen to be around -40 dB and in the right diagram, around -100 dB. Similarly the magnitude of the returned signal can be read, and thus the SNR can be determined simply with $SNR = A_{signal,dB} - A_{noise,dB}$.

As can be seen above circled on the figures, the ball is thrown up and arcs down towards a person catching it. Thus 1 represents the high initial velocity of the ball

being thrown, then the ball decreases linearly in velocity as expected as it experiences only constant negative acceleration due to gravity. At 1.5 seconds it moves beyond the beam angle of the transducer (2 in the figure) and is caught at around 1.7 seconds. The signals at 2 seconds and 3 seconds are likely the swinging of the player's arms after throwing the ball. Similarly, below the evident path of the ball, microdopplers can possibly be observed of slower moving body parts of the player and spin of the ball.

Hereafter, a threshold is applied to the received signal to remove noise and the signal is normalized, producing the following results:

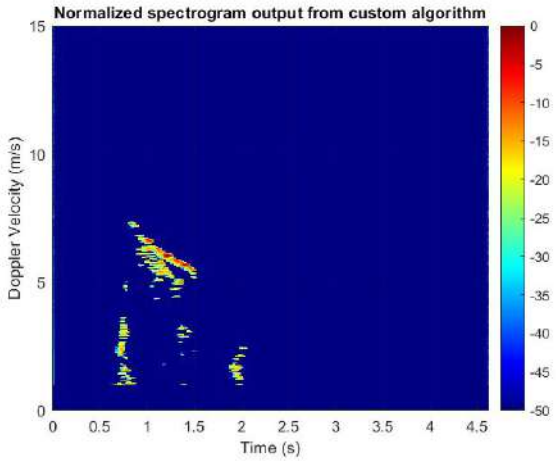

Figure 5.5: Normalized custom spectrogram output

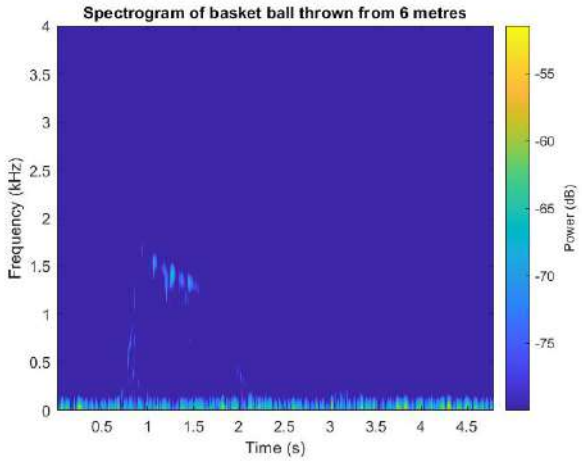

Figure 5.6: Normalized pspectrum output

In the above figures it can be seen that the noise is significantly reduced with most microdopplers being removed as well, making it easier to extract velocity. It is worth noting that the pspectrum approach produces a much cleaner spectrogram without having to tune any parameters for any environment, devoid of noise and unnecessary low power returns. Finally, the velocity is extracted as shown below:

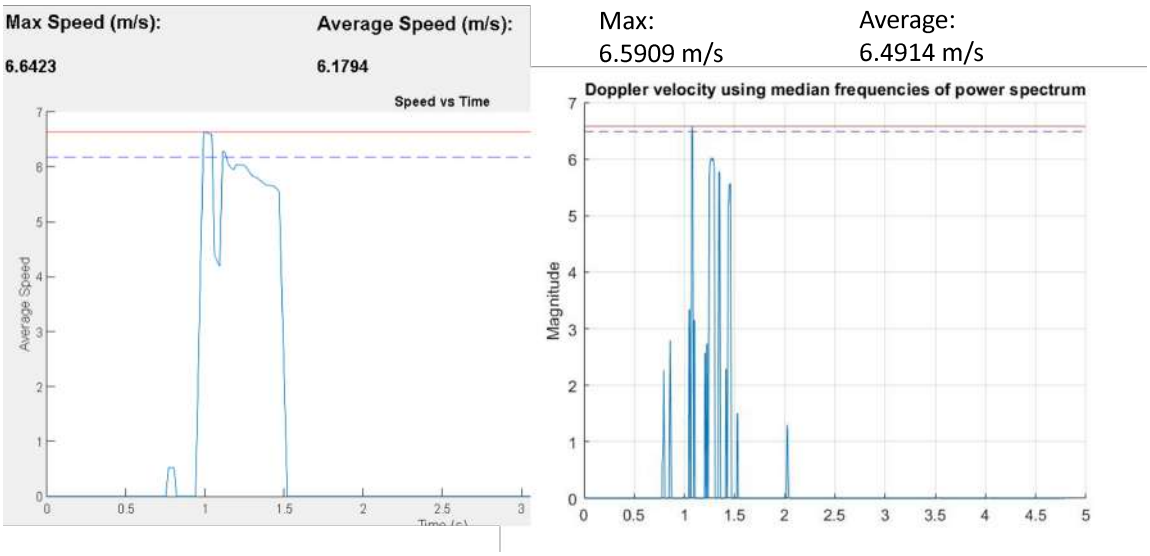

Figure 5.7: Velocity metrics outputted from both processing methods

The velocity data is extracted and smoothed and plotted. The custom STFT shows a smoother instantaneous velocity graph however due to smoothing some information is lost such as the random dip in the trend. The mean, taken as a moving window across the data seems accurate given the result. The pspectrum result, using the median frequencies from the power spectrum, produces an accurate result but the graph of velocity is less user-friendly however shows more information. Regarding the video data, the time that the ball is released from the hands of the player is recorded along with the time that the ball passes the radar. Thus a time of flight can be recorded along with the distance which is set by markers within the video. This specific example provided the following results:

- Video:
  Vavg $= 7.5 \pm 1.13$ m/s
- Custom STFT:
  Vavg $= 6.18 \pm 0.87$ m/s
  Vmax $= 6.64 \pm 0.87$ m/s
- MedFreq approach:

Vavg = 6.49 ± 0.87 m/s
Vmax = 6.59 ± 0.87 m/s

Uncertainties were calculated as follows:
Video data:

- Uncertainty of time, u(T) = $\sqrt{[\frac{0.01}{2\sqrt{3}}]^2 + 2[0.1 * T]^2}$
- Uncertainty of distance, u(D) = $\sqrt{[\frac{0.2}{2\sqrt{6}}]^2 + [0.05 * D]^2}$
- Uncertainty of speed, u(Vavg) = $Vavg\sqrt{[\frac{u(D)}{D}]^2 + [\frac{u(D)}{D}]^2}$

In the time uncertainty calculation, 10% of the time was propagated as error due to the uncertainty in reading the time frames from the video data. Furthermore, this digital measurement used 5.1. Distance uncertainty included an analogue instrument (tape measure) and thus used 5.2. 5% error was included in the uncertainty due to inaccuracies of markers and reading off distance correctly from video data. Similar calculations were then carried out for ultrasonic measurements as well. A table of all results including uncertainties is shown in the Appendix in A.2.

These results were then compared in an interval, and as is observable above, agree within a reasonable degree of uncertainty, and the custom STFT and medFreq results agree with each other as well. In this way, all results were obtained and compared.

5.1.3 Results Summary

The video data provided velocity measurements, as did the custom velocity estimation algorithm (see A.2) as well as the 'medfreq' approach (see A.3). 'Outdoor Tests' below shows a 4th comparison - 'Video vs Custom 2' - this is for the custom velocity estimation algorithm with altered parameters.

The indoor and outdoor test results are summarized below (see A.2 Appendix for a more detailed example of how collected data looked):

Table 5.1: Table of frequency tests

Varied Frequency Testing		
Frequency	Video vs Audio	SNR (dB)
8.00	Yes	45
10.00	Yes	20
12.00	Yes	20
14.00	No	20
Frequency	Video vs Ultra	dB
38.00	No	20
39.00	Yes	20
39.50	Yes	23
40.00	Yes	30

Table 5.2: Table of range tests

Range Tests		
Ball	Ultrasonic Range (m)	Audio Range (m)
Basket Ball	8.5	Indoor - 2.5
Footballl	8	Indoor - 2.5
Tennis	Indoor - 2.5	Indoor - 2.5
Squash	Indoor - 2.5	Indoor - 2.5

Table 5.3: Table of indoor test results

Indoor Tests				
Ball	Video vs Ultra Custom	Video vs Ultra Med Freq	Video vs Audio	Custom vs Med Freq
Rugby	100%	100%	100%	100%
Tennis	100%	100%	67%	100%
Squash	67%	100%	100%	100%

Table 5.4: Table of outdoor (slower ball speed) test results

Outdoor Tests 2						
Ball	Video vs Ultra Custom	Video vs Ultra Med Freq	Video vs Audio	Custom vs Med Freq	Video vs Custom 2	Video vs S-Band RADAR
Basket Ball	100%	100%	67%	100%	100%	N/A
Football	0%	67%	0%	0%	67%	100%
Tennis	0%	0%	0%	100%	0%	100%
Squash	0%	0%	0%	100%	0%	N/A

5.2 Discussion

5.2.1 Frequency Tests

The important results to acknowledge first are the frequency tests - the ultrasonic results were expected with a transmitting frequency of 40 kHz being optimal with the greatest SNR of 30 dB. As expected, the SNR decreased as the centre frequency of the signal moved out of the bandwidth of the transducer. The audio tests however produced a surprising result. 8 kHz seems to be the optimal frequency to use at an SNR of 45 dB but a frequency of 12 kHz was used for tests. This poses an avenue for improving the performance of the audio system.

5.2.2 Noise Threshold

The noise threshold for each system was determined via the calibration function and thereafter fine tuned experimentally. Whilst the calibration function may produce a threshold of -10 dB in one outdoor scenario, eventually the threshold of -20 dB was used for outdoor tests for the custom STFT method. For the case of the pspectrum and median frequency approach, a noise threshold of -80 dB proved adequate for all situations and was quite reliable.

5.2.3 Optimal Algorithm Tests

Firstly observing the indoor tests in 5.3, all algorithms showed good performance classifying all balls of all sizes relatively well from distances up to 2.5 metres. The custom STFT algorithm misclassified some squash ball speeds but came close, as they agreed within uncertainty limits with the median frequency result 100% of the time.

Hereafter, looking at the outdoor test results in 5.4, one can immediately observe the high success rate of the median frequency algorithm versus the custom STFT algorithm. For basket balls, both algorithms performed well but for footballs the median frequency algorithm had a higher rate of success in determining the correct speeds of the balls. It was then observed that adjusting parameters of the spectrogram (2^{10} samples per frame and 0.7% frame overlap) in the custom algorithm produced similar success rates as shown in "Video vs Custom 2" in 5.4.

Pairing the results of the indoor tests with the outdoor tests and the fact that the pspectrum function needed no adjustment to work in whatever environment proved it to be the superior algorithm for extracting velocity metrics. Whilst the instantaneous velocity produced is not ideal as shown in 5.7, this can be improved with a smoothing function. As a result, the medfreq algorithm was then used to test the audio system as well.

Despite adjusting parameters and taking numerous tests, either algorithm did not classify speeds of smaller balls well like tennis and squash balls. This will be further discussed in the RCS tests section.

5.2.4 Ball Size (RCS) Tests

Indoor tests showed that all sizes of balls from rugby balls to squash balls (30 cm to 4 cm) could be accurately detected and the speed thereof estimated within 2.5 metres. However, as the testing moved outdoors to longer ranges, the performance dropped off. Basket balls could be reliably measured with the ultrasonic system and

the audio system showed mixed success. Footballs showed mixed success with the ultrasonic system and no success with the audio system. From here, as the RCS decreased dramatically to that of a tennis and squash ball, both systems could not accurately estimate the speeds of the balls. As shown in 2.6, as the cross sectional area of a reflector decreases, the power returned decreases, and thus the magnitude of the STFT would be lower and thus less in contrast to the surrounding noise in a spectrogram, see 5.4. The low power returned from the reduced RCS of the balls together with an algorithm under test and high noise meant the system was not sensitive enough to pick up the balls' speeds. However, more tests would give a more rigorous conclusion to what size balls can be accurately measured.

On the other hand, the S-Band MIT Coffee Can RADAR was able to accurately measure speeds of over 20 m/s for footballs and smaller RCS objects such as tennis balls and cricket balls. More detailed results for this system can be seen in A.1 and A.2. This is a possible indicator of why RF systems are typically favoured for sports applications such as these.

5.2.5 Range Tests

These range results were determined by cross referencing video frames with spectrogram outputs, and comparing the time on the spectrogram when the ball is visible, to the time in the video and reading the distance marker off of that. Thus, the range tests may vary in accuracy however offer a reasonable benchmark that agrees with the velocity estimation accuracy of the system and the expected range as a result of the RCS of the balls and signal power decreasing exponentially over distance. Range results for the S-Band Coffee Can RADAR could not be reliably compiled from given data as the video was recorded on looking the ball instead of a profile view from which distances can be better observed.

In 5.2 one can see that basket balls with the greatest RCS could be first accurately picked up by the ultrasonic system at 8.5 metres. Footballs at 8 metres, and tennis and squash balls could not be accurately measured outdoors but indoors, a range of

2.5 metres was possible. For the audio tests, whilst the ball's velocity was visible on the spectrogram, the velocity could not be successfully extracted and thus the audio has a range of 2.5 metres for all balls as measured indoors.

5.3 Acceptance Test Procedures Evaluation

- ATP001: Range Tests
  This was discussed in Range Tests 5.2.5 previously where the device could accurately estimate the velocity of large sports balls like basket balls and footballs from 8 metres. Smaller balls like tennis and squash balls were only able to be accurately measured from 2.5 metres indoors. Thus ATP001 was passed with mixed success.

- ATP002: MATLAB GUI for user
  As shown in 5.3, once recording is finished, the velocity metrics are displayed to the user, passing ATP002.

- ATP003: Enclosure for device
  In the Design section of this report at 4.24 the finished enclosure is shown, meeting ATP003.

- ATP004: Transmit and receive in various environments
  Indoor and outdoor tests were carried out with varying levels of success depending on ball size. See 5.1.1. ATP004 was passed.

- ATP005: PC-Based System
  All tests were carried out with the XONAR U5 connected to a laptop running the MATLAB GUI as shown in the experiment setup 5.1.1, thus passing ATP005.

- ATP006: User friendly Interface
  The developed MATLAB GUI is extremely simple with instructions included as well. Assistants during experiments could easily operate software. ATP006

was thus passed.

- ATP007: Velocity accuracy test
  Object speeds were estimated with RADAR and video data and compared. ATP007 was passed with mixed success, primarily with objects with large RCS to a maximum range of 8.5 metres.

- ATP008: +-12V Supply Rails
  The design in 4.19 correctly produced +-12V allowing the LT1214CN opamps in the Tx and Rx circuits to be powered correctly, passing ATP008.

Chapter 6

Conclusions

6.1 Conclusions

A PC-based ultrasonic radar system was designed from the ground up to measure an object's speed for indoor and outdoor sports training and research purposes. The system was well packaged, low cost and came with a user friendly application to record sports activities. The maximum, average and instantaneous velocity of basket balls and footballs was accurately estimated and displayed whilst smaller balls had mixed success. The success rate of an audio system and S-Band RF system were compared as well, thus meeting the objectives outlined in 1.3.

This research project was able to determine the effectiveness of using ultrasonic and audio systems as viable solutions for estimating the velocity of sports balls for sports training purposes. The system was also developed to allow for further development later, including space in the enclosure to allow it to be developed into a standalone system instead of being PC-based. The developer software also allowed the system to operate with customized parameters. The ultrasonic system was also developed within a low budget of R860.00 as seen in A.1.

The ultrasonic and audio systems were found to accurately estimate the speed of sports balls of most sizes indoors within a range of 2.5 metres. Outdoors in the

desired scenario, the audio system did not operate effectively being unable to accurately estimate the speed of sports balls reliably. The ultrasonic system however showed better performance accurately estimating the speed of basket balls and footballs (objects with large RCS) up to ranges of 8.5 and 8 metres respectively. The ultrasonic system was unable to accurately estimate the speed of smaller balls (tennis and squash) outdoors. Tests with higher velocity balls showed lower rates of success with speeds over 12 m/s, reflecting the hypothesis that the narrow bandwidth of the ultrasonic transducers would limit the maximum observable speeds of the system - due to the reduced observable range of Doppler frequencies. Frequencies higher than 42 kHz would be significantly attenuated and thus not distinguished amongst noise in the spectrum when received.

This research project showed that ultrasonic and audio technology can be applied to velocity estimation of sports balls with mixed success compared to the typical RF approach. Whilst the ultrasonic system was unable to estimate speeds over 12 m/s, the system can be improved as discussed in the recommendations, and would be possibly viable for primary school level sports ball measurement. It further showed an improvement over that of an audio system for the same application. The developed ultrasonic and audio systems would further be useful as a low budget option for students investigating RADAR technology and gain hands-on experience. The system as a whole has a lot of room for improvement as discussed next.

6.2 Future Work

6.2.1 Hardware

The ultrasonic system could be developed into a standalone unit instead of being PC-based. A DSP, ADC/DAC and display (an 8 segment display would be adequate) would need to be added and Tx, Rx and power supply circuits developed into PCBs. MATLAB code can be exported in C code and run on the DSP. The whole unit can then be reduced in size by using rechargeable Li-ion cells instead of a power bank and then redesigning a smaller enclosure for the embedded system.

The hardware and further be improved by reducing noise it introduces into the system. Low Dropout (LDO) regulators can be added to the +-12V rails in the power circuitry to reduce switching noise from the MT3608 boost converter. Size of decoupling capacitors need to be considered in case they are introducing oscillations. AUX cables should be ensured to be shielded.

6.2.2 Software

The system can be expanded to operate in live situations where the STFT is processed and the velocity estimated repeatedly, thus allowing the system to be left on and displaying speeds as balls pass by. The speed can be displayed until cleared or hold for a few seconds then continue operating. Additionally, for a PC-based system, implementing a rolling waterfall FFT to display a live spectrogram could prove useful.

6.2.3 RADAR system

The research project investigated a CW ultrasonic RADAR to estimate the velocity of objects - work can thus also be done investigating the viability of ultrasonic FMCW and Pulse-Doppler RADARs for the same application.

Furthermore, the ultrasonic system was unable to measure speeds over 10 m/s due to the narrow bandwidth of the transducer. Emitting at 40 kHz, with a bandwidth of 2 kHz, Doppler frequencies of greater than 2 kHz were significantly attenuated thus limiting the range of speeds that could be measured. This can be improved by transmitting at 38 kHz and boosting the signal significantly. The speed of sports balls is unlikely to be lower than 3 m/s in general and thus higher velocities would be received in the optimal frequency range for the ultrasonic system (40-42 kHz would correspond to higher velocities). By setting the centre frequency to 38 kHz one can improve the range of velocities that can be measured to likely 18 m/s.

The audio system was found to operate with a higher SNR at 8 kHz instead of 12 kHz, thus the system could be found to have greater accuracy if tested at this centre frequency. Thus the ultrasonic and audio RADAR systems have room for improvement.

6.2.4 Signal Processing

The current system conducts key signal processing steps as described in 4.27 and then applies a threshold with a small amount of smoothing. This process of extracting the object from the spectrum can be improved with more advanced techniques such as using a tracking algorithm with an alpha-beta filter. Furthermore, if enough data is collected, an LSTM Neural Network or Optical Flow with a Convolutional Neural Network (CNN) could use RADAR results to train and learn to predict velocity estimates via supervised learning.

6.2.5 Experimentation

Many more experiments could be carried out to expand the data set to rigorously identify what balls can be measured with what velocity at what ranges with reduced uncertainty. This can be improved by using an accurate sports Doppler RADAR (such as a pocketRADAR) to compare results against. Furthermore, max speed results can be investigated with pendulum motion from which max speeds can be reliably determined. Lastly, the audio system should be tested at 8 kHz which was found to be the optimal carrier frequency for increasing SNR when detecting sports balls.

Bibliography

[1] M. Richards, J. Scheer, J. Scheer, and W. Holm, *Principles of Modern Radar: Basic Principles, Volume 1*, ser. Electromagnetics and Radar. Institution of Engineering and Technology, 2010. [Online]. Available: https://books.google.co.za/books?id=nD7tGAAACAAJ

[2] "pocket radar personal ball coach radar gun." [Online]. Available: https://www.athleticstuff.com/pocket-radar-personal-ball-coach-radar-gun/

[3] "Buyer's guide to sport velocity-tracking devices," 2018. [Online]. Available: https://simplifaster.com/articles/buyers-guide-sport-velocity-tracking-devices/

[4] "what we track." [Online]. Available: https://trackmangolf.com/what-we-track

[5] B. Shanker and J. Fuchs, "A precision radar for performance athletes." [Online]. Available: https://snt-highlights.uni.lu/2021/04/06/a-precision-radar-for-performance-athletes/

[6] C.-s. Lin, M. Yunus, A. Gaffar, J. Son, and S. Winberg, "Dynamic Hand Gesture Recognition using Doppler Sonar and Deep Learning," Ph.D. dissertation, University of Cape Town, 2021.

[7] A. Makanjee and E. Engineering, "Generating synthetic radar data of a golf shot for a Doppler simulator," Ph.D. dissertation, University of Cape Town, Cape Town, 2020.

[8] L. Alonso, V. Milan, C. Torre-Ferrero, J. Godoy, J. P. Oria, and T. De Pedro, "Ultrasonic sensors in urban traffic driving-aid systems," *Sensors*, vol. 11, no. 1, pp. 661–673, 2011.

[9] J. Martin, "Evaluation of doppler radar ball tracking and its experimental uses," Ph.D. dissertation, Washington State University, 2012.

[10] Curry, "Synthetic Aperture Sonar for 2D imaging," Ph.D. dissertation, University of Cape Town, 2019.

[11] R. O'Donnell, "Introduction to radar systems," 2021.

[12] "Radar during world war ii - engineering and technology history," 2021. [Online]. Available: https://ethw.org/Radar_during_World_War_II

[13] "The history of the radar gun," 2021. [Online]. Available: https://www.efastball.com/history/history-of-the-sports-radar-gun/

[14] "classic inventions - inspirations - sable accelerator network," 2021. [Online]. Available: https://www.sablenetwork.com/inspirations/classic/14

[15] . G. Tischler, "80 ghz radar vs. ultrasonic: Non-contact level measurement technology comparison," Nov 2019. [Online]. Available: https://www.automation.com/getattachment/685571b1-e5f1-4a80-9187-96a9ef2ad622/WhitePaper_80GHz_vs_Ultrasonic.pdf?lang=en-US&ext=.pdf

[16] A. Carovac, F. Smajlovic, and D. Junozovic, "Application of ultrasound in medicine," 2011. [Online]. Available: https://www.ncbi.nlm.nih.gov/pmc/articles/PMC3564184/

[17] A. Tedeschi, S. Calcaterra, and F. Benedetto, "Ultrasonic radar system (uras): Arduino and virtual reality for a light-free mapping of indoor environments," *IEEE Sensors Journal*, vol. 17, no. 14, pp. 4595–4604, 2017.

[18] "Applications for ultrasonic sensors 2021," 2021. [Online]. Available: https://www.pepperl-fuchs.com/southafrica/en/32702.htm

[19] R. Li, S. Kling, M. Salata, S. Cupp, J. Sheehan, and J. Voos, "Wearable performance devices in sports medicine," 2016. [Online]. Available: https://www.ncbi.nlm.nih.gov/pmc/articles/PMC4702159/

[20] J. Mons, "6 great ways how sensors are positively transforming sports," 2021. [Online]. Available: https://sporttomorrow.com/how-sensors-are-transforming-the-world-of-sports/#1_The_data_generator%E2%80%A6

[21] "Hawk-eye." [Online]. Available: https://www.hawkeyeinnovations.com/

[22] A. Ghosh, "Application of hawk-eye technology in sports," 2019. [Online]. Available: https://www.techentice.com/application-of-hawk-eye-technology-in-sports/

[23] A. Gudipudi, "Detection and velocity of a fast moving object," Ph.D. dissertation, Blekinge Institute of Technology, 2021.

[24] K. Kaur, "Electronic sensors in sports to monitor performance," 2013. [Online]. Available: https://www.azosensors.com/article.aspx?ArticleID=151

[25] W. P. Du Plessis, "Audio Sonar for Gaining Hands-On Experience of Radar Principles," *IEEE National Radar Conference - Proceedings*, vol. 2020-September, pp. 2020–2022, 2020.

[26] A. Bodenstein, *S-band radar detection of targets in outdoor sporting applications.* University of Cape Town, 2020.

[27] "Fastest moving ball sport." [Online]. Available: https://www.guinnessworldrecords.com/world-records/fastest-moving-ball-sport

Appendix A

Supporting Data

Table A.1: Bill of materials for ultrasonic system

Part type	**Supplier**	**Value**	**Quantity**	**Single or pack**	**Unit Price (incl VAT)**	**Total**
Resistor	RS Components	12 kΩ	9	Pack of 10	0.669	6.69
Resistor	RS Components	120 kΩ	2	Pack of 10	0.779	7.79
Resistor	RS Components	1 kΩ	2	Single	4.34	8.68
Capacitor (electrolytic or pol)	RS Components	10 pF	2	Single	10.79	21.58
Capacitor (electrolytic or pol)	RS Components	100 pF	3	Pack of 10	4.76	47.3
Capacitor (electrolytic or pol)	RS Components	15 nF	1	Pack of 5	3.903	19.515
Capacitor (electrolytic or pol)	RS Components	150 pF	1	Pack of 10	3.973	39.73
Capacitor (electrolytic or pol)	RS Components	3.3 pF	2	Single	24.38	48.76
Capacitor (electrolytic or pol)	RS Components	1 nF	1	Single	14.82	14.82
Capacitor (electrolytic or pol)	RS Components	330 pF	2	Single	13.39	26.78

Capacitor (electrolytic or pol)	RS Components	220 pF	1	Single	24.26	24.26
Capacitor (electrolytic or pol)	RS Components	47 pF	1	Single	22.53	22.53
Capacitor (electrolytic or pol)	RS Components	68 pF	1	Pack of 10	5.34	53.4
Capacitor (electrolytic or pol)	RS Components	22 pF	1	Single	11.76	11.76
Polarized (Coupling) Capacitor	RS Components	100 nF	1	Single	3.48	3.48
Schottkey Diode	RS Components	1N5819	2		9.76	19.52
Potentiometer	RS Components	10 kΩ	3	Single	14.5	43.5
Op amp	RS Components	LT1214CN	2 x quad	Single	202.46	404.92
3D printed PLA enclosure	UCT Mechatronics Lab	-	1	-	-	-
Male 2.54 mm header	UCT White Lab	-	24	-	-	-
Female to female jumper cables	UCT White Lab	-	17	-	-	-
Ultrasonic Barrel Transmitter	UCT White Lab	-	1	-	-	-
Ultrasonic Barrel Receiver	UCT White Lab	-	1	-	-	-
Switch	UCT White Lab	-	1	-	-	-
Red LED	UCT White Lab	-	1	-	-	-
Audio jack socket	UCT White Lab	-	2	-	-	-
12/5V Mini car battery charger	Dr Yunus Abdul Gaffar	-	1	-	-	-
Car battery jumper cable	Dr Yunus Abdul Gaffar	-	2	-	-	-
5mm self tapping screw	Gordan's Tool & Hardware	-	4	-	30	30
Total			77			R855.015

Table A.2: Outdoor test results (2nd custom results omitted for neatness)

Ball	D (m)	u(D)	T (s)	u(T)	Vavg	u(Vavg)	Ultra Vavg (custom)	Ultra Vmax (custom)	Ultra Vavg (medfreq)	Ultra Vmax (medfreq)	u(V)
Basket Ball	6.00	0.303	0.80	0.113	7.50	1.13	6.57	7.20	6.46	6.56	0.866
Basket Ball	10.00	0.502	1.24	0.175	8.10	1.22	7.33	7.33	6.78	6.78	0.866
Soccer	6.00	0.303	0.83	0.118	7.19	1.08	16.34	16.44	5.34	5.95	0.866
Soccer	10.00	0.502	1.17	0.165	8.58	1.29	34.32	34.33	5.71	5.73	0.866
Soccer	10.00	0.502	1.27	0.179	7.88	1.18	16.37	16.38	7.27	7.31	0.866
Tennis	6.00	0.303	0.87	0.123	6.92	1.04	1.23	1.45	0.00	0.00	0.866
Tennis	10.00	0.502	1.10	0.156	9.09	1.36	0.00	0.00	0.00	0.00	0.866
Squash	6.00	0.303	0.87	0.123	6.92	1.04	2.55	2.66	2.35	2.61	0.866
Squash	10.00	0.502	1.17	0.165	8.55	1.28	0.00	0.00	0.00	0.00	0.866

Penalty kick experiments	Time at maximum speed (seconds)	Maximum recorded speed (m/s)	Time travelled (seconds)	Distance travelled (metres)	Calculated speed (m/s)
Radar placed behind net:					
Test 1	2	15	0.33	4.9	14.8
Test 2	0.5	17	0.32	4.9	15.3
Radar placed behind player:					
Test 3	1.3	15	0.6	8.7	14.5
Test 4	2.4	17	0.51	8.7	17.1

Figure A.1: S-Band Radar football test results

Description	Time at service recorded by radar (seconds)	Maximum recorded speed (m/s)	Time travelled (seconds)	Distance travelled (metres)	Calculated speed (m/s)
Tennis serve test 1:					
Ball 1	2.0	28	0.64	18.50	28.9
Ball 2	6.4	25	0.65	18.40	28.34

Figure A.2: S-Band Radar tennis ball test results

See all code at the following repository: Ultrasonic Radar repository

Listing A.1: Signal Processing code to return Doppler frequencies at baseband

```
%% Author: Ian Edwards
%The function processes data for a CW Doppler RADAR operating at carrier
%frequency Fc_Hz. It produces all the Doppler frequencies from a received
%signal.

function [TxSignal, data, data_bpf, data_notch, data_shifted, data_out, t] = processDoppler(Fs, Fc_Hz, TimeDuration_s, TxSignal, data)
    c = 343; % [m/s]  ->speed of sound wave
    Ts = 1/Fs; % Sampling period
    t = 0:Ts:(TimeDuration_s) % time vector for pulse

    % Fs -> Sample rate [Hz]
    % Fc_Hz -> Carrier Frequency [Hz]
    % Time_Duration_s -> Transmit time (signal duration)
    % Tx_Signal -> Transmitted signal
    % data -> Received signal
    %-------------------------------------------------------
    %Shifted over by 0.2 seconds because there is a delay from transmission to
    %receiving. Received signal comes in 0.2 seconds later.
    start = 0.2/(1/Fs);
    TxSignal = TxSignal(start:end-1);
    data = data(start:end-1);
    t = 0.2:Ts:TimeDuration_s;
    N = length(t);
    %-------------------------------------------------------
```

```
25      %% Process received signal into usable format
26      % Remove DC offset and noise around DC with BPF - dont
            want it shifted when we
27      % baseband shift.
28      % First Passband Frequency make this Fc - 0.554*Fc
29      Fpass1 = Fc_Hz-0.554*Fc_Hz;
30      % First Stopband Frequency Fpass1 - 100
31      Fstop1 = Fpass1 - 100;
32      % Second Passband Frequency make this Fc + 0.554*Fc
33      Fpass2 = Fc_Hz+0.554*Fc_Hz;
34      % Second Stopband Frequency make this Fpass2 + 100
35      Fstop2 = Fpass2 + 100;
36
37      [b,a] = butter(6, [Fstop1 Fstop2]/(Fs/2),'bandpass');
38      data_bpf = filter(b,a, data);
39
40      %-----------------------------------------------------
41      % Create notch filter around Fc_Hz to remove clutter.
42      % creating notch filter coeficcients:
43      w0=Fc_Hz/(Fs/2);
44      bw=w0/1000;
45      [b,a]=iirnotch(w0,bw);
46
47      data_notch = data_bpf - mean(data_bpf);
48      data_notch = filter(b,a, data_notch);
49      %-----------------------------------------------------
50      % base band shift signal. DC offset has been removed.
51      data_shifted = Baseband(data_notch, Fc_Hz, Fs, 0);
52
53      % Down sample since only frequencies close to 0 Hz are
            relevant now.
54      data_out = downsample(data_shifted, 8);
```

```
55 end
```

Listing A.2: Code for custom method of obtaining ball velocity estimations

```
1  function [max_v, avg_v, instant_v] = getVelocities(app, t_s,
       f, v_factor, S)
2      %Calculate velocities (max, avg, instantaneous)
3      max_frequencies = zeros(length(t_s),1);
4      for frame = 1:length(t_s)
5          %gets max STFT magnitude in frame.
6          [max_S, index] = max(S(:, frame));
7           %if higher than threshold and frequency is not
                higher than realistically observable
8          if (max_S >= app.threshold) && (f(index) < app.
               TransmitFrequencyHzEditField.Value/4)
9              %store corresponding frequency value
10             max_frequencies(frame) = f(index);
11         else
12             max_frequencies(frame) = 0;
13         end
14     end
15     instant_v = max_frequencies*v_factor;
16     instant_v = smoothdata(instant_v,'movmean',3);
17     max_v = max(instant_v);
18     %obtain mean as a moving window across the data
19     avg_v = max(movmean(instant_v, 5));
20 end
```

Listing A.3: Code for the "Medfreq" method of obtaining ball velocity estimations

```
1 [P1,F,T]=pspectrum(data_out,Fs/8,'spectrogram','
    FrequencyResolution',128, 'FrequencyLimits',[0 4000],'
    MinThreshold',app.pthreshold);
2 figure;
```

```
3  pspectrum(data_out,Fs/8,'spectrogram','FrequencyResolution'
       ,128, 'FrequencyLimits',[0 4000], 'MinThreshold',app.
       pthreshold);
4  title("Spectrogram of basket ball thrown from 6 metres");
5  %Extract median frequencies
6  freqs = medfreq(P1, F);
7  %Convert Doppler frequency to velocity
8  dv1 = freqs * v_factor;
9  for i = 1:length(dv1)
10     if dv1(i) < 1
11         dv1(i) = 0;
12     end
13 end
14 %Smooth a small amount to remove noise spikes
15 dv1= smoothdata(dv1,'movmean',2);
16 max_speed = max(dv1,[],'omitnan');
17 %small moving window because of jittery nature of returns
18 avg = max(movmean(dv1, 2, 'omitnan'));
```